DEUTSCHES ELEKTRONEN-SYNCHROTRON **DESY**

DESY 86-084
August 1986

CUMULATIVE BEAM BREAKUP IN LARGE-SCALE LINACS

by

K. Yokoya

Deutsches Elektronen-Synchrotron DESY, Hamburg

and

National Lab. for High Energy Physics, KEK, Tsukuba, Japan

ISSN 0418-9833

NOTKESTRASSE 85 · 2 HAMBURG 52

To be sure that your preprints are promptly included in the
HIGH ENERGY PHYSICS INDEX ,
send them to the following address (if possible by air mail) :

DESY
Bibliothek
Notkestrasse 85
2 Hamburg 52
Germany

DESY 86-084
August 1986

ISSN 0418-9833

CUMULATIVE BEAM BREAKUP IN LARGE-SCALE LINACS

KAORU YOKOYA

Deutsches Elektronen-Synchrotron DESY, Hamburg

National Laboratory for High Energy Physics, Japan

ABSTRACT

The cumulative transverse beam breakup in large linacs such as the ones for linear colliders is discussed. Various analytic formulae are derived which allow arbitrary initial condition, focussing and acceleration. The spread in the mode frequency can be taken into account. The misalignment problem is also discussed.

Typeset by $\mathcal{A}_{\mathcal{M}}\mathcal{S}$-TEX

1. Introduction

It is said that the most promising candidate of the high energy electron-positron collider in the next generation is a linear collider. Several new acceleration mechanisms giving the field gradient of more than a hundred MeV/m have been proposed. Nevertheless, the conventional RF acceleration seems to be feasible up to the energy somewhere around 1 TeV, although much effort should be made for the development of the high-power microwave generator. Such a large linac is expected to require extremely large power. One possible way to save power is to put many bunches in one RF pulse in contrast to the SLC, where one pulse consists of only three bunches (including both electron and positron). This also relaxes the problem of the beamstrahlung during the collision because the charge per bunch can be small. One of the major problem of such a linac in multi-bunch operation is the so-called cumulative beam breakup. The single bunch instability is not so serious because of the low charge per bunch. The multi-bunch mode gives nearly the same luminosity as the single-bunch if the charge per bunch is divided by the square root of the number of bunches, whereas the total charge per pulse is multiplied by the same factor.

The mechanism of the cumulative beam breakup in linacs can be stated as follows. If a bunch in a pulse is displaced from the central axis of the linac due to some reason, it excites a transverse deflecting mode in the cavity, such as the HEM_{11} mode. The following bunches feel this field in the same cavity and are deflected even if they are on the axis. These deflected bunches create fields of the same type in the cavities in the rest of the linac, which further deflect the subsequent bunches leading to a beam loss.

This problem has been studied by several authors. Helm and Loew (ref.1) discussed the problem by an analytic method for linacs with no or weak focussing. Neil, Hall and Cooper (ref.2) gave an exact solution and an asymptotic analytic expression for the periodic focussing structure with no acceleration, putting the emphasis mainly on high-intensity, low energy linacs. Gluckstern, Cooper and Channell (ref.3) treated the problem more rigorously and derived the steady state solution for a long pulse with some discussions on the acceleration. In all these works, only one deflecting mode of the cavities is taken into account and the beam offset from the machine axis at the injection was discussed as the source of the trigger of the deflecting mode excitation.

The linacs for linear colliders have some different features which have not yet been treated in these works. There, the acceleration is very important (the adiabatic damping factor amounts to several tens) and the focussing structure inevitably changes as the beam is accelerated. It is impossible to maintain the same optics in the low and the high energy portions of the linac because of the large energy difference. This is even unnecessary because beam breakup is more serious in the low energy portion. Since the number of the accelerating and focussing elements is large, the misalignments of these elements are also important as the trigger of the breakup. Another complication comes from the fact that we may use cavities of various types which have slightly different deflecting mode frequencies in order to damp the

breakup by dephasing. This is expected to be a powerful cure to cumulative beam breakup. We already have the same situation for constant-gradient type cavities. The frequency of one deflecting mode of the cavity of this type has a spread over a finite frequency band.

On the other hand there are also some points which make our study easy. The local details of the focussing and accelerating structures are of less importance. They can be characterized by a few numbers such as the betatron wave length and the impedance per unit length. The spacings of the quadrupole magnets and the cavities do not play an important role. They can be smoothed out. One more good news is that the focussing should be very strong so that the breakup during one betatron wavelength is small. Otherwise, we cannot accelerate the beam through many betatron wavelengths.

In this circumstance, we prefer an approximate but analytic treatment rather than the exact, discrete methods such as matrices and recurrence relations. Our method is based on the one employed in ref.1. It is very flexible and can handle the various possibilities stated above.

In Section 2 we formulate the problem of the initial beam offset and derive an approximate integral representation of the solution. It is applied to the beam breakup by isolated deflecting modes in Section 3, and extended to the case of the frequency spread in Section 4. Section 5 and 6 deal with the problem of the misalignments of the cavities and the quadrupole magnets, respectively. The main results are summarized in Section 7. Appendix A discusses the single-bunch blowup by the same formalism and Appendix B gives the steady state solution. Appendix C and D are mathematical notes for Section 4.

2. Beam Offset at Injection

In Sections 2 to 4 we discuss the problem of the beam offset at the injection. In this section we derive an approximate integral representation of the beam breakup factor in a general form which allows arbitrary initial condition, acceleration, focusing and cavity impedance. It will be employed in the later sections. The method was basically first introduced by R.Helm and G.Loew in ref.1.

Let $x_j(s)$ be the transverse coordinate (we consider only one transverse plane) of the j-th bunch when it passes the point s, the length along the linac measured from the injection point. We treat the bunches as point charges. We approximate the focusing structure by a smooth focusing function $k(s) = 2\pi/(\text{local betatron wave length})$. It can be a slowly varying function of s so as to allow the change of the optics from low energy to high energy. We assume that every bunch has the same electric charge. Then the equation of motion of the i-th bunch is

$$\frac{d}{ds}\left(\gamma(s)\frac{dx_j}{ds}\right) + \gamma(s)k(s)^2 x_j(s) = \frac{eIt_b}{mc^2}\sum_{k=0}^{j} W(t_j - t_k)x_k(s). \tag{2.1}$$

Here, the notation is:

$\gamma(s)$ the beam energy in the unit of the rest energy mc^2. It is assumed to be a slowly varying function of s. We treat untrarelativistic particles only.

t_b the bunch spacing (in the unit of time). We define $\omega_b = 2\pi/t_b$. Every RF bucket need not be filled but the bunch spacing must be equal.

I the average beam current. The charge of a bunch is given by $I \cdot t_b$.

t_j $= jt_b$, the time delay of the j-th bunch from the first (zeroth) bunch.

$W(t)$ the transverse dipole wake potential by a unit charge per unit length of the linac in units of Volt/m^2/Coulomb. We assume the "causality" $W(t) = 0$ for $t < 0$. We ignore the short-term variation of $W(t)$ with s due to the various structures along the linac. We do not consider the possible long-term variation by using cavities of different types in the low and high energy parts. The latter possibility is not difficult to take into account in our formalism.

If necessary, the effect of alternating focusing in the real linac can easily be taken into account approximately. To do so, we write the local amplitude functiuon $\beta(s)$ in the form $\beta_{osc}(s)/k(s)$. Here, $\beta_{osc}(s)$ is a dimensionless function with unit average, showing the short-period oscillation of the beta function. Use $x_i(s)/\sqrt{\beta_{osc}(s)}$ instead of $x_i(s)$ and redefine s by $\int_0^s ds/\beta_{osc}(s)$. Then one finds that one should multiply $W(t)$ by β_{osc}^2 with β_{osc} being the average value of $\beta_{osc}(s)$ in the cavities.

Let us define the (discrete) Laplace transform of $x_j(s)$ with respect to j;

$$y(s,p) = t_b \sum_{j=0}^{\infty} e^{-pt_j} x_j(s) \qquad (\Re p > p_c). \tag{2.2}$$

Here, p_c is the convergence coordinate, which we do not know yet. This equation defines $y(s,p)$ in the region $\Re p > p_c$, where y is analytic. For $\Re p < p_c$, $y(s,p)$ is defined by the analytic continuation. The Laplace transform $y(s,p)$ has the periodicity

$$y(s, p + i\omega_b) = y(s,p). \tag{2.3}$$

The inverse of (2.2) is given by

$$x_j(s) = \frac{1}{2\pi i} \int_{-i\omega_b/2+p_c}^{+i\omega_b/2+p_c} dp\, e^{pt_j} y(s,p) dp, \tag{2.4}$$

where p_c must be so chosen that every singularity of $y(s,p)$ is to the left of p_c.

Using $y(s,p)$, eq(2.1) can be written as

$$\frac{d}{ds}\left(\gamma(s)\frac{dy}{ds}\right) + \gamma(s)k(s)^2 y(s,p) = \frac{eIt_b}{mc^2} y(s,p) \sum_{j=0}^{\infty} e^{-pt_j} W(t_j). \tag{2.5}$$

We introduce the impedance $\hat{Z}$ corresponding to $W(t)$;

$$\hat{Z}(ip) = -it_b \sum_{j=0}^{\infty} e^{-pt_j} W(t_j) \qquad \Re p > p_c. \tag{2.6}$$

Thus, eq(2.1) reduces to an ordinary differential equation for each p;

$$\frac{d}{ds}\Big(\gamma(s)\frac{dy}{ds}\Big) + \gamma(s)\Big[k(s)^2 - \frac{\hat{V}(p)}{\gamma(s)}\Big]y(s,p) = 0, \tag{2.7}$$

with

$$\hat{V}(p) = \frac{eI}{mc^2} i\hat{Z}(ip). \tag{2.8}$$

These variable have the same periodicity in p as (2.3);

$$\hat{V}(p + i\omega_b) = \hat{V}(p), \qquad \hat{Z}(i(p + i\omega_b)) = \hat{Z}(ip). \tag{2.9}$$

Since we assume that the s-dependence of $k(s)$ and $\gamma(s)$ is moderate, we can use WKB approximation in solving eq(2.7). The principal solution is

$$y_{\pm}(s,p) = \Big[\gamma^2(k^2 - \frac{\hat{V}}{\gamma})\Big]^{-1/4} \exp\Big[\pm i \int_0^s \sqrt{k^2 - \frac{\hat{V}}{\gamma}}\, ds\Big]. \tag{2.10}$$

We further approximate this expression by the assumption that the focusing is strong. It holds if the beam breakup during one betatron wave length is small. This is the case in high energy linacs where the total number of betatron oscillation is large. The opposite case of weak focusing has been discussed in ref.1. Thus, eq(2.10) can be approximated by

$$y_{\pm}(s,p) = \frac{1}{\sqrt{\gamma(s)k(s)}} \exp\Big[\pm i \int_0^s (k - \frac{\hat{V}}{2k\gamma}) ds\Big]. \tag{2.11}$$

Introducing the phase function of the betatron oscillation

$$\psi(s) = \int_0^s k(s) ds \tag{2.12}$$

and a function

$$H(s) = \int_0^s \frac{ds}{\gamma(s)k(s)}, \tag{2.13}$$

we can write eq(2.10) as

$$y_{\pm}(s,p) = \frac{1}{\sqrt{\gamma(s)k(s)}} \exp \pm i\Big[\psi(s) - \frac{1}{2}H(s)\hat{V}(p)\Big]. \tag{2.14}$$

Now, let us consider the initial condition. If the initial values of $x_j(s)$ and $x_j'(s)$ at $s=0$ for all j are given, then the initial values of y and y' are calculated by

$$y(0,p) = t_b \sum_{j=0}^{\infty} e^{-pt_j} x_j(0), \qquad y'(0,p) = t_b \sum_{j=0}^{\infty} e^{-pt_j} x_j'(0). \tag{2.15}$$

For instance, when every bunch is injected with the same offset X_0 without slope, (2.15) gives

$$y(0,p) = \frac{X_0 t_b}{1-e^{-pt_b}} \qquad \text{and} \qquad y'(0,p) = 0. \tag{2.16}$$

If only the first bunch is displaced by X_0 and the others are on the axis, we have

$$y(0,p) = X_0 t_b \qquad \text{and} \qquad y'(0,p) = 0. \tag{2.17}$$

The linear combination of y_+ and y_- that satisfies (2.15) is given by

$$y(s,p) = \sqrt{\frac{\gamma_0 k_0}{\gamma(s)k(s)}}\left[y(0,p)\cos\Big(\psi(s) - \frac{1}{2}H(s)\hat{V}(p)\Big) + \frac{y'(0,p)}{k_0}\sin\Big(\psi(s) - \frac{1}{2}H(s)\hat{V}(p)\Big)\right], \tag{2.18}$$

where $\gamma_0 = \gamma(0)$ and $k_0 = k(0)$.

We get an integral representation of $x_j(s)$ by the inverse Laplace transformation (2.4);

$$x_j(s) = \sqrt{\frac{\gamma_0 k_0}{\gamma k}} \sum_{\pm} \frac{1}{4\pi i} \int_{-i\omega_b/2+p_c}^{+i\omega_b/2+p_c} dp\Big[y(0,p) \pm \frac{y'(0,p)}{ik_0}\Big] e^{\pm i\left(\psi(s) - \frac{1}{2}H(s)\hat{V}(p)\right) + pt_j}. \tag{2.19}$$

Since $\hat{V}(p)^* = \hat{V}(p^*)$, which states the wake potential $W(t_j)$ is real, we can simplify (2.19) as

$$x(s,t) = \sqrt{\frac{\gamma_0 k_0}{\gamma(s)k(s)}} \Re \frac{e^{i\psi(s)}}{2\pi i} \int_{-i\omega_b/2+p_c}^{+i\omega_b/2+p_c} \tilde{y}(0,p) e^{\hat{\varphi}(p)} dp \tag{2.20}$$

with

$$\hat{\varphi}(p) = pt - \frac{i}{2}H(s)\hat{V}(p) \tag{2.21}$$

and

$$\tilde{y}(0,p) = y(0,p) + \frac{y'(0,p)}{ik_0}. \tag{2.22}$$

Here, $\Re$ denotes the real part. Eq(2.20) makes sense only for t a multiple of t_b and, then, $x_j(s)$ is given by $x(s,t_j)$.

Now, if we know the impedance, the focusing function and the initial condition, we can estimate the beam blowup factor by integrating the expression (2.20).

In practice, it is not easy to carry out the integral (2.20) because the integrand is much involved and the interval of the integration is finite. However, we can get a crude approximation in the following manner. We usually define the transverse impedance by

$$W(t) = \frac{i}{2\pi}\int_{-\infty}^{+\infty} Z(\omega)e^{-i\omega t}d\omega, \qquad Z(\omega) = -i\int_{-\infty}^{+\infty} W(t)e^{i\omega t}dt. \tag{2.23}$$

One finds that Z and $\hat{Z}$ have the relation

$$\hat{Z}(ip) = \sum_{n=-\infty}^{\infty} Z(ip + n\omega_b). \tag{2.24}$$

It is evident that the impedance $Z(\omega)$ and $Z(\omega + n\omega_b)$, n being an integer, give the same $\hat{Z}$. Therefore, we may redefine $Z(ip)$ by properly shifting the argument by $in\omega_b$ so that $Z(ip)$ has a singularity only in the region

$$-\frac{\omega_b}{2} \leq \Im p < +\frac{\omega_b}{2}. \tag{2.25}$$

(Sometimes, the interval $(0, \omega_b)$ is better.) Even if $Z(ip)$ has several singularities, we can often decompose $Z(ip)$ and shift the argument for each component. This prescription may fail in some special cases, e.g., a long branch cut which extends over more than ω_b in the imaginary direction.

If, in the integral (2.20), we can ignore the contribution of the singularities outside this region, we may replace $\hat{\varphi}(p)$ in (2.20) with $\varphi(p)$ defined by

$$\varphi(p) = pt - \frac{i}{2} H(s) V(p), \tag{2.26}$$

where $V(p)$ is given by (2.8) with $\hat{Z}$ replaced by Z;

$$V(p) = \frac{eI}{mc^2} iZ(ip). \tag{2.27}$$

Furthermore, if $Z(ip)$ is smooth enough outside the region (2.25) and if t is large enough, we may extend the integration interval to infinity because the contribution of the region outside (2.25) is cancelled out owing to the rapid oscillation of the factor e^{pt} in $\varphi(p)$. Thus, we have

$$x(s,t) = \sqrt{\frac{\gamma_0 k_0}{\gamma(s) k(s)}} \Re \frac{e^{i\psi(s)}}{2\pi i} \int_{-i\infty+p_c}^{+i\infty+p_c} \tilde{y}(0,p) e^{\varphi(p)}. \tag{2.28}$$

The formula (2.28) is quite powerful but must be used very carefully.

The same formalism can be used for the problem of the single-bunch breakup. This is much simpler than our problem because one can use the continuous Laplace transformation. This is briefly described in Appendix A.

3. Beam Breakup by an Isolated Deflecting Mode

In this section we carry out the integral (2.20) for the case of one single resonant mode of the cavities. The results can also be applied to a realistic case where several modes exist, provided their frequencies are well separated from each other in the sense described below. The wake potential of a deflecting mode can be written in the form

$$W(t) = W_0 e^{-\epsilon t} \sin \omega_0 t. \tag{3.1}$$

In the commonly used notation, the parameters W_0 and ε are written as $W_0 = R\omega_0/Q$ and $\varepsilon = \omega_0/2Q$ (We ignore $1/Q^2$.), where Q is the quality factor, ω_0 the resonant angular frequency and R the shunt impedance per unit length in units of ohm/m^2. (In practice, R (and W_o) must be reduced a little from the value of real cavities in order to take into account the dilution by the other elements such as focusing magnets and drift spaces.) In this paper we use W_0 and ε instead of R and Q for the following reason. As one can see from the equation of motion (2.1), only the values of the wake potential at $t =$ multiple of t_b contribute in our problem. Therefore, the resonant frequency $\omega_0 + n\omega_b$ ($n =$ integer) should give the same results as ω_0; i.e., ω_0 makes sense up to modulo ω_b. We denote the smallest one among them by $[\omega_0]$ ($|[\omega_0]| < \omega_b/2$). Therefore, $[\omega_0]$ can be negative and it expresses the distance from the nearest bunch spectrum $n\omega_b$. On the other hand, the original value of ω_0 must be kept in $R\omega_0/Q$ and in $\omega_0/2Q$, which may cause confusion. So, we prefer W_0 and ε.

The impedance (2.23) corresponding to (3.1) is given by

$$Z(ip) = \frac{W_0}{2}\Big(\frac{1}{p + i\omega_0 + \varepsilon} - \frac{1}{p - i\omega_0 + \varepsilon}\Big). \tag{3.2}$$

As stated in Section 2, this impedance gives the same $\hat{Z}$ as

$$Z(ip) = \frac{W_0}{2}\Big(\frac{1}{p + i[\omega_0] + \varepsilon} - \frac{1}{p - i[\omega_0] + \varepsilon}\Big) \tag{3.3}$$

does. We shall use the latter form, which has poles only in the region (2.25).

Let us estimate the integral appearing in (2.20);

$$\hat{F}(s,t) = \frac{1}{2\pi i}\int_{-i\omega_b/2+p_c}^{+i\omega_b/2+p_c} \tilde{y}(0,p)e^{\hat{\varphi}(p)}dp \tag{3.4}$$

with

$$\hat{\varphi}(p) = pt + \frac{eIH(s)}{2mc^2}\hat{Z}(ip) = pt + \frac{\Omega(s)}{4}\sum_{n=-\infty}^{\infty}\Big(\frac{1}{p + i[\omega_0] + in\omega_b + \varepsilon} - \frac{1}{p - i[\omega_0] + in\omega_b + \varepsilon}\Big), \tag{3.5}$$

and

$$\Omega(s) = \frac{eIH(s)W_0}{mc^2} = \frac{eIW_0}{mc^2}\int_0^s \frac{ds}{\gamma(s)k(s)}. \tag{3.6}$$

Here, $\Omega(s)$ has a dimension of frequency and is a monotonically increasing function of s. It will play an important role thoughout this paper. If the focusing function $k(s)$ is constant and the acceleration is uniform, then

$$\Omega(s) = \frac{eIW_0}{k(dE/ds)}\log\frac{\gamma(s)}{\gamma_0}, \tag{3.7}$$

where dE/ds is the (smoothed) acceleration gradient. The expression (3.5) has poles at $p = \pm i[\omega_0] + in\omega_b$. If ω_0 is not very close to the middle between successive multiples of ω_b,

or, equivalently, if $|\omega_0|/\omega_b$ is not very close to $\pm 1/2$, we may ignore the interference between the poles of different n. Then, instead of (3.4) and (3.5), we may use

$$F(s,t) = \frac{1}{2\pi i}\int_{-i\infty+p_c}^{+i\infty+p_c} \hat{y}(0,p)e^{\varphi(p)}dp \tag{3.8}$$

with

$$\varphi(p) = pt + \frac{elH(s)}{2mc^2}Z(ip) = pt + \frac{\Omega(s)}{4}\Big(\frac{1}{p+i|\omega_0|+\varepsilon} - \frac{1}{p-i|\omega_0|+\varepsilon}\Big), \tag{3.9}$$

which is regular outside the region (2.25). We can obtain $x(s,t)$ by (2.28).

Since we are not much interested in the front part of the pulse where the blowup is not serious, we may assume large t in (3.8) so that the saddle point method can be applied. The saddle points are solutions of the equation

$$\varphi'(p) = t - \frac{\Omega(s)}{4}\Big(\frac{1}{(p+i|\omega_0|+\varepsilon)^2} - \frac{1}{(p-i|\omega_0|+\varepsilon)^2}\Big) = 0. \tag{3.10}$$

If $|\omega_0|$ is not too small, the interference between the two poles near $-\varepsilon \pm i|\omega_0|$ can be ignored and the saddle points are given by

$$\begin{aligned} p_1 &= -\varepsilon - i|\omega_0| + \frac{1}{2}\sqrt{\frac{\Omega(s)}{t}}, \qquad p_2 = -\varepsilon - i|\omega_0| - \frac{1}{2}\sqrt{\frac{\Omega(s)}{t}}, \\ p_3 &= -\varepsilon + i|\omega_0| + \frac{i}{2}\sqrt{\frac{\Omega(s)}{t}}, \qquad p_4 = -\varepsilon + i|\omega_0| - \frac{i}{2}\sqrt{\frac{\Omega(s)}{t}}. \end{aligned} \tag{3.11}$$

When there are two mode frequencies at the distance $\delta\omega_0$, the condition that they do not interfere can be expressed as

$$t \gg \frac{\Omega(s)}{2(\delta\omega_0)^2}. \tag{3.12}$$

Thus, we assume that both

$$\delta\omega_0 = 2|\omega_0| \qquad \text{and} \qquad \delta\omega_0 = \omega_b - 2|\omega_0| \tag{3.13}$$

are not close to zero so as to satisfy (3.12). The latter is the nearest distance between the poles of different n. In practice, the region of ω_0 where (3.12) fails is very small.

When several deflecting modes coexist, we may ignore the interference between the modes if

$$\delta\omega_0 = |\omega_0^{(a)}| - |\omega_0^{(b)}|, \tag{3.14}$$

satisfies (3.12). Here $\omega_0^{(a)}$ is the frequency of the a-th mode. Then we can consider each mode separately. Bear in mind that $\delta\omega_0$ is not simply $\omega_0^{(a)} - \omega_0^{(b)}$.

The four roots of (3.10) are depicted in the complex p-plane in Fig.1. The integration path must be to the right of the singularities (poles at $p = -\varepsilon \pm i|\omega_0|$). One can see from (3.5) that the rightmost saddle point p_1 dominates in the integral when t is large. Since

$$\varphi(p_1) = -\varepsilon t - i|\omega_0|t + \sqrt{\Omega(s)t} \tag{3.15}$$

and $\Re\varphi(p_{3,4}) = -\varepsilon t$, the condition that the other saddle points can be ignored is[1]

$$\Re\varphi(p_1) - \Re\varphi(p_3) = \sqrt{\Omega(s)t} \gg 1. \tag{3.16}$$

The two conditions (3.12) and (3.16) can be combined to

$$\frac{1}{t} \ll \Omega(s) \ll 2(\delta\omega_0)^2 t. \tag{3.17}$$

Near the saddle point p_1, the function $\varphi(p)$ can be approximated by

$$\varphi(p) = \varphi(p_1) + \frac{1}{2}(p - p_1)^2\varphi''(p_1) \tag{3.18}$$

with

$$\varphi''(p_1) = \frac{4t\sqrt{t}}{\sqrt{\Omega(s)}}. \tag{3.19}$$

The initial value $\tilde{y}(0,p)$ in (3.8) can be replaced with its value at $p = p_1 \cong -\varepsilon - i|\omega_0|$. When t is so large that $\varepsilon t - \sqrt{\Omega(s)t} \gg 1$, all the saddle points are to the left of the imaginary axis. Hence, the contributions of these saddle points die away as $t \to \infty$. On the other hand, $\tilde{y}(0,p)$ may have poles on the imaginary axis. For example, if the beam is modulated by a frequency ω_{in} at the injection, $\tilde{y}(0,p)$ has poles at $p = \pm i|\omega_{in}|$. (The initial condition (2.16) is the special case of $\omega_{in} = 0$.) The contribution of these poles is finite at $t \to \infty$. Therefore, when one is interested in the steady state at $t \to \infty$, one cannot ignore the contribution of the poles of $\tilde{y}(0,p)$. This is not important for linear colliders but, for completeness, it is briefly described in Appendix B. Here, we ignore these poles. So, the following formulae are valid under the condition

$$\sqrt{\Omega(s)t} - \varepsilon t \gg 1. \tag{3.20}$$

Thus, we can perform the integral (3.8) with the result

$$F(s,t) = \frac{1}{2\sqrt{2\pi}}\tilde{y}(0, -\varepsilon - i|\omega_0|)\left(\frac{\Omega(s)}{t^3}\right)^{1/4} e^{-\varepsilon t - i|\omega_0|t + \sqrt{\Omega(s)t}}. \tag{3.21}$$

Therefore, substituting this expression into (2.28), we obtain

$$x(s,t) = \frac{1}{2\sqrt{2\pi}}\sqrt{\frac{\gamma_0 k_0}{\gamma(s)k(s)}}\left(\frac{\Omega(s)}{t^3}\right)^{1/4} \Re\tilde{y}(0, -\varepsilon - i|\omega_0|)e^{-\varepsilon t - i|\omega_0|t + i\psi(s) + \sqrt{\Omega(s)t}}. \tag{3.22}$$

The oscillation amplitude is

$$X(s,t) = \frac{1}{2\sqrt{2\pi}}\sqrt{\frac{\gamma_0 k_0}{\gamma k}}\left(\frac{\Omega(s)}{t^3}\right)^{1/4} e^{-\varepsilon t + \sqrt{\Omega(s)t}}|\tilde{y}(0, -\varepsilon - i|\omega_0|)|. \tag{3.23}$$

[1] If we neglect the interference between the poles, we can integrate (3.8) exactly for each pole using the Bessel function of order one (J_1 or I_1 according to the sign of the residue of the pole) without the assumption (3.16). However, this does not help much because the resulting expressions are rather involved and, moreover, the only merit is that they also apply to the small blowup part of the beam, which we are not interested in.

For the initial condition (2.16) and (2.17), we get

$$X(s,t) = \frac{X_0}{2\sqrt{2\pi}}\sqrt{\frac{\gamma_0 k_0}{\gamma k}}(\Omega(s)t)^{1/4}\frac{t_b}{t}e^{-\varepsilon t+\sqrt{\Omega(s)t}}\left\{\begin{array}{c}\left[(e^{\varepsilon t_b}-1)^2+4e^{\varepsilon t_b}(\sin\frac{\omega_0 t_b}{2})^2\right]^{-1/2}\\ 1\end{array}\right\} \tag{3.24}$$

where the upper and lower part in the curly bracket correspond to (2.16) and (2.17), respectively. The initial condition (2.16) leads to a resonance when $\omega_0 t_b$ is a multiple of 2π as seen from the upper factor. Eq(3.22) is the main result of this section. It can describe the behavior of the beam under the conditions (3.17) and (3.20). One can get the solution for arbitrary initial condition $x_j(0)$ and $x_j'(0)$ by calculating their 'Laplace component' $y(0,-i[\omega_0])$ and $y'(0,-i[\omega_0])$ and substituting them into (3.22). When more than one deflecting mode come in, one can simply sum the contribution of each mode to $x(s,t)$, if the separations between the mode frequencies, (3.14), are large enough to satisfy (3.12).

The breakup is essentially described by the factor $\exp(\sqrt{\Omega(s)t})$. In the case of no acceleration and constant optics, this agrees with the result in ref.2. The maximum blowup takes place at the end of the pulse $t = T$ and at the exit of the linac $s = L$ (neglecting the factor $e^{-\varepsilon t}$). As one can see from the definition of $\Omega(s)$, (3.6), this factor $\exp(\sqrt{\Omega(L)T})$ is determined by the total charge in the pulse but does not depend on the bunch spacing (apart from the resonance phenomena).

Fig.2 to 5 show the comparison with a computer tracking. We solved the equation of motion (2.1) by the Runge-Kutta method in s. The acceleration is uniform and the focusing function is constant. The following parameters are used throughout this paper as the standard values, otherwise stated. Eq(2.17) is used for the initial condition (offset of the first bunch only).

$t_b = 10\,\text{nsec}$ $\quad(\omega_b = 2\pi \times 100\,\text{MHz})$

$n_b = 50$ $\quad$(number of bunches)

$L = 2000\,\text{m}$

$\omega_0 = 2\pi \times 4.214\,\text{GHz}$ $\quad[\omega_0] = 0.14\omega_b$

$mc^2\gamma_0 = 2\,\text{GeV}$

$d(mc^2\gamma(s))/ds = 0.1\,\text{GeV/m}$

$k(s) = 0.10\,\text{m}^{-1}$

$I \cdot t_b = 3.2\,\text{nC}$

$W_0 = 1.4 \times 10^{15}\,\text{volt/C/m}^2$

$\varepsilon = 0$ $\quad(Q \to \infty)$

$\Delta\omega = 2\pi \times 6\,\text{MHz}$ $\quad$(for Sectin 4)

These parameters give

$$\Omega(s) = 2\pi \times 7.1\,\log(1+\frac{s}{20m}) \qquad (\text{MHz}).$$

The integration step is 2m.

Fig.2a and 2b show an example of $x(s,t)/X_0$ as a function of time (bunch index) given by the tracking and eq(3.22), respectively. In Fig.3 to 5, shown is the logarithm of the amplitude or, more specifically, $\log_{10}(\bar{X}(s,t)/X_0)$ where $\bar{X}$ is the "invariant" amplitude, i.e.,

$$\bar{X}(s,t) = \sqrt{\frac{\gamma(s)k(s)}{\gamma_0 k_0}} X(s,t). \tag{3.25}$$

There is some difficulty in defining the amplitude in the computer tracking. We defined it by

$$X(s,t_j) = \sqrt{x_j^2(s) + (x_j'(s)/k(s))^2},$$

which, rigorously speaking, cannot compare with the analytic formulae, e.g., (3.23), when the breakup is very fast. The crosses show the results of tracking and the solid lines the analytic formula (3.24). The amplitude is plotted as a function of t in Fig.3 and as a function of s in Fig.4. One finds slight disagreements between the analytic formula and the tracking in the region of small s and t, where the condition (3.17) is not fulfulled. Fig.5 shows the resonance between the mode frequency and the bunch frequency. Here, $[\omega_0]$ is varied from the standard value. The horizontal axis is the fractional part of ω_0/ω_b. The initial condition (2.16) (offset of all the bunches) was used for this plot. The resonance is described by the upper factor in the curly brackets in eq(3.24). The formula (3.24) agrees with the tracking fairly well even near the resonance, though a small error is seen near $[\omega_0]/\omega_b = \pm 1/2$. In all cases, Fig.2 to 5, our analytical formula (3.22) (or (3.23)) shows excellent agreements with the tracking except where the blowup is insignificant.

4. The Frequency Spread

We have considered the case of mutually isolated deflecting modes in the previous section, but in practice, the modes are more complicated in cavities of the constant gradient type. The resonant frequency of one deflecting mode is a function of the location in the cavity unit. Such a mode can approximately be described by many modes each of which has slightly different frequency. Under such a circumstance we may expect a damping of the beam breakup phenomena because of the dephasing by the frequency spread. Even if the 'natural' spread in frequencies in constant-gradient-type cavities is not sufficient, we can design a linac consisting of slightly different type cavities with the same accelerating frequency but different deflecting mode frequencies. The aim of this section is to find the required frequency spread to damp the cumulative beam breakup.

The impedance of such structures can be written as

$$Z(ip) = \sum_a \frac{W_0^{(a)}}{2} \left[\frac{1}{p + i[\omega_0]^{(a)} + \varepsilon^{(a)}} - \frac{1}{p - i[\omega_0]^{(a)} + \varepsilon^{(a)}} \right]. \tag{4.1}$$

Under the same assumption as in the previous section, we use the simplified formulae (2.23) to (2.28) in this section, too, instead of (2.20) and (2.21). In practice, each mode is asociated with a different place in the linac but we ignore this fact and treat it as if all the modes are excited in every cavity. We shall assume that all the modes in the frequency band have the same W_0 and ε and that they are uniformly distributed in the region $([\omega_0]-\frac{1}{2}\Delta\omega, [\omega_0]+\frac{1}{2}\Delta\omega)$. We further assume that the number of the frequencies in the band, n_f, is so large that the sum in (4.1) can be replaced by an integral over ω_0. The required number of frequencies for this assumption to hold can be given by the opposite inequality of (3.12);

$$\frac{\Delta\omega}{n_f} \ll \sqrt{\frac{\Omega(s)}{t}}, \tag{4.2}$$

but this criterion is too crude to apply to practical problems such as how many types of cavities are needed. It should be determined by computer tracking.

As we stated in the previous section, ω_0 makes sense only up to modulo ω_b. If $\Delta\omega$ is large and ω_0/ω_b is close to an integer, the frequency interval $([\omega_0]-\frac{1}{2}\Delta\omega, [\omega_0]+\frac{1}{2}\Delta\omega)$ may contain a multiple of ω_b. We do not consider such a case and assume $\frac{1}{2}\Delta\omega < |[\omega_0]|$. Otherwise, we cannot confine the singularities in the region (2.25) so that the simplified formulae (2.23) to (2.28) cannot be applied.

With these assumptions we can rewrite the impedance (4.1) as

$$Z(ip) = \frac{W_0}{2i\Delta\omega}\left[\log\frac{p+\varepsilon+i([\omega_0]+\frac{1}{2}\Delta\omega)}{p+\varepsilon+i([\omega_0]-\frac{1}{2}\Delta\omega)} + \log\frac{p+\varepsilon-i([\omega_0]+\frac{1}{2}\Delta\omega)}{p+\varepsilon-i([\omega_0]-\frac{1}{2}\Delta\omega)}\right], \tag{4.3}$$

where W_0 is not the wake amplitude of one mode frequency but the sum of all the modes in the band. As in the previous section, if t and/or $|[\omega_0]|$ is large (i.e., far away from the resonance) so that the condition (3.12) holds, then the second term in the square brackets in (4.3) can be ignored. Substituting (4.3) into (2.27), we get

$$\varphi(p) = pt + \frac{\Omega(s)}{4i\Delta\omega}\log\frac{p+\varepsilon+i([\omega_0]+\frac{1}{2}\Delta\omega)}{p+\varepsilon+i([\omega_0]-\frac{1}{2}\Delta\omega)}, \tag{4.4}$$

where the same expression as in the previous section, (3.7), is understood for $\Omega(s)$. Since only the vicinity of $p = -\varepsilon - i[\omega_0]$ contributes in the integral (2.28), we can replace $\tilde{y}(0,p)$ by $\tilde{y}(0,-\varepsilon-i[\omega_0]) \cong \tilde{y}(0,-i[\omega_0])$. (Here, we shall not consider the steady state at $t\to\infty$. See Appendix B.) The integral

$$F(s,t) = \frac{1}{2\pi i}\int_{-i\infty+p_c}^{+i\infty+p_c} e^{\varphi(p)}dp, \tag{4.5}$$

$\varphi(p)$ being given by (4.4), is evaluated in Appendix C. Here we quote only the assumptions and the results. In addition to the assumptions (3.17) and (3.20), we assume

$$\frac{\Omega(s)}{\Delta\omega} \gtrsim 1. \tag{4.6}$$

(The resulting formulae is valid for finite Q (nonzero ϵ) but we shall omit the factor $e^{-\epsilon t}$ in the following discussion except (4.8) because we are mainly interested in the beam behavior for t less than the cavity filling time.)

The result can be written in the form;

$$x(s,t) = X(s,t)\cos\Big(\psi(s) - [\omega_0]t + \arg\tilde{y}(0,-\epsilon - i[\omega_0])\Big) \tag{4.7}$$

with

$$X(s,t) = \sqrt{\frac{\gamma_0 k_0}{\gamma(s)k(s)}}|\tilde{y}(0,-\epsilon - i[\omega_0])|\frac{1}{t}\sqrt{\frac{2\Omega(s)}{\Delta\omega}}\Big[\frac{\varsigma}{1-\frac{\Omega(s)}{t(\Delta\omega)^2}}\Big]^{1/4} e^{-\epsilon t}\sinh(\frac{\pi\Omega(s)}{4\Delta\omega})\mathbf{Ai}(-\varsigma), \tag{4.8}$$

where

$$\begin{aligned}
\varsigma &= +\Big[\frac{3}{4}\int_{\frac{\Omega(s)}{\Delta\omega^2}}^{t}\Delta\omega dt\sqrt{1-\frac{\Omega(s)}{t(\Delta\omega)^2}}\Big]^{2/3} \\
&= +\Big[\frac{3}{4}\Big(-\frac{\Omega(s)}{\Delta\omega}\cosh^{-1}\sqrt{\frac{t(\Delta\omega)^2}{\Omega(s)}} + \sqrt{(t\Delta\omega)^2-\Omega(s)t}\Big)\Big]^{2/3} \qquad t(\Delta\omega)^2 > \Omega(s) \\
&= -\Big[\frac{3}{4}\int_{t}^{\frac{\Omega(s)}{\Delta\omega^2}}\Delta\omega dt\sqrt{\frac{\Omega(s)}{t(\Delta\omega)^2}-1}\Big]^{2/3} \\
&= -\Big[\frac{3}{4}\Big(+\frac{\Omega(s)}{\Delta\omega}\cos^{-1}\sqrt{\frac{t(\Delta\omega)^2}{\Omega(s)}} - \sqrt{\Omega(s)t-(t\Delta\omega)^2}\Big)\Big]^{2/3} \qquad t(\Delta\omega)^2 < \Omega(s)
\end{aligned} \tag{4.9}$$

Here, for convenience, the definition of $X(s,t)$ allows negative values. The factor in the fourth root in (4.8) is always positive and smooth at the zero of the denominator. The important factors in (4.8) are the last two; i.e., hyperbolic sine and $\mathbf{Ai}(-\varsigma)$. Here, $\mathbf{Ai}(-\varsigma)$ is Airy's function, which can be expressed by the Bessel functions of order one third. It is plotted in Fig.14 and some formulae concerning it are summarized in Appendix D. The essential feature of $\mathbf{Ai}(-\varsigma)$ is that, for $\varsigma > 0$, it is an oscillatory function with the amplitude decreasing with ς and that it is exponential-like for $\varsigma < 0$ and decays rapidly as $\varsigma \to -\infty$. The relation between t,$\Omega(s)$ and ς is depicted in Fig.6, where the contours of constant ς are drawn on the $(t\Delta\omega,\Omega(s)/\Delta\omega)$ plane. Note that $\Omega(s)$ is a monotonically increasing function of s (linear for constant energy and logarithmic for uniform acceleration, if $k(s)$ is constant). The dashed lines show the zeroes of $\mathbf{Ai}(-\varsigma)$ and the solid line the maximum. One sees that $X(s,t)$ (not $x(s,t)$) is oscillatory in the region of large t and small Ω (small s) and exponential for small t and large Ω.

The asymptotic forms of $\mathbf{Ai}(-\varsigma)$ for $\varsigma \to \pm\infty$ are given in Appendix D, eqs(D.5) and (D.6). Using these expressions we obtain the asymptotic forms of the amplitude $X(s,t)$; in

the exponential region

$$X(s,t) = \sqrt{\frac{\gamma_0 k_0}{\gamma k}} |\tilde{y}(0,-i[\omega_0])| \frac{1}{2\sqrt{2\pi t}} \Big[\frac{\Omega^2 t}{\Omega - t\Delta\omega^2}\Big]^{1/4} (1 - e^{-\frac{\pi\Omega}{2\Delta\omega}}) \\ \times \exp\Big[\frac{\Omega}{2\Delta\omega} \sin^{-1}\sqrt{\frac{t\Delta\omega^2}{\Omega}} + \frac{1}{2}\sqrt{\Omega t - (t\Delta\omega)^2}\Big] \quad (\varsigma \ll -1) \tag{4.10}$$

and in the oscillatory region

$$X(s,t) = \sqrt{\frac{\gamma_0 k_0}{\gamma k}} |\tilde{y}(0,-i[\omega_0])| \frac{1}{t}\sqrt{\frac{2}{\pi}} \sinh(\frac{\pi\Omega}{4\Delta\omega}) \\ \times \sin\Big[-\frac{\Omega}{2\Delta\omega} \cosh^{-1}\sqrt{\frac{t\Delta\omega^2}{\Omega}} + \frac{1}{2}\sqrt{(t\Delta\omega)^2 - \Omega t} + \frac{\pi}{4}\Big] \quad (\varsigma \gg 1). \tag{4.11}$$

In the transition region $\varsigma \sim 0$ ($\Omega \sim t\Delta\omega^2$) we have to use (4.7). One easily finds that (4.10) agrees with the result of the previous section, eq(3.23), in the limit of no frequency spread $\Delta\omega \to 0$. In this case one sees only the exponential region. The amplitude $X(s,t)$ (actually $|X(s,t)/X_0|$) is depicted in Fig.7 as a two-argument function. Fig.7a and 7b are the results of the tracking and the formula (4.8), respectively. The s-axis is linear in $\Omega(s)$. The bunch index is shown instead of the time t. The frequency spread is $\Delta\omega = 2\pi \times 6$ MHz. One can clearly see the first zero and the maximum of $\mathbf{Ai}(-\varsigma)$ in either figure.

Fig.8 shows $x(s,t)$ as a function of t (bunch index) for fixed s. The displacement $x(s,t)/X_0$ by tracking is shown in Fig.8a and the same quantity by the formula (4.7) is plotted in Fig.8b. The short oscillation period is determined by the fractional part of $[\omega_0]/\omega_b$ (=0.14 in our exmple). The shift of the phase by π when crossing a zero of Airy's function can clearly be seen in both figures. Their agreement is excellent. Fig.8c, shows the amplitude $|\tilde{X}(s,t)/X_0|$. The crosses are the results of the tracking and the solid line shows eq(4.8). The relative error near the zeroes of $\mathbf{Ai}(-\varsigma)$ is large because the ignored terms can play a role there, but this is not important for our purpose. In all cases, our analytic formulae show good agreements with the tracking in the portion of the beam of large blowup, which we are mostly interested in.

Now, consider the following practical problem: "How large is the maximum amplitude of the oscillation in the given linac length L and the given pulse length T?" The behavior of $X(s,t)$ as a function of s with fixed t is as follows (see Fig.6 and 7 along a vertical line). It is oscillatory for small s, becoming larger as s increases, and comes into transition region when $\Omega(s) \sim t\Delta\omega^2$. It stops oscillating in the exponential region and rapidly increases. Therefore, the maximum amplitude occurs at the exit of the linac $s = L$. The behavior of $X(s,t)$ as a function of t is different (see Fig.8c). It increases exponentially for small t, takes a maximum in the transition region $t \sim \Omega(s)/\Delta\omega^2$ and starts oscillating with decreasing amplitude. This behavior mainly comes from Airy's function. The maximum occurs at the point close to the maximum of Airy's function $\mathbf{Ai}(-\varsigma)$; i.e., $\varsigma \approx 1.02$, $\mathbf{Ai} \approx 0.536$. In practice this value of ς is

not as important as that of **Ai**. So, for simplicity we regard that $\mathbf{Ai}(-\varsigma)$ takes the maximum 0.536 at $\varsigma \approx 0$; i.e., at $t \approx \Omega(s)/\Delta\omega^2$.

If the frequency spread $\Delta\omega$ is too small or the pulse length is too short, this maximum (and, therefore, the succeeding damp) does not occur within the given length of the pulse. In such cases the spread does not cause significant damping of the cumulative beam breakup. The condition that the maximum occurs within the pulse length is

$$\Delta\omega \gtrsim \sqrt{\frac{\Omega(s)}{T}}. \tag{4.12}$$

At $\varsigma \sim 0$ ($t \sim \Omega/\Delta\omega^2$), the factor in the fourth root in eq(4.8) becomes

$$\lim_{\varsigma \to 0} \frac{\varsigma}{1 - \Omega(s)/t\Delta\omega^2} = \left(\frac{\Omega(s)}{2\Delta\omega}\right)^{2/3}. \tag{4.13}$$

Therefore, when (4.12) holds, $X(s,t)$ takes the maximum at $s = L$ and $t \approx \Omega(L)/\Delta\omega^2$

$$X_{max} \approx 0.536\sqrt{\frac{\gamma_0 k_0}{\gamma(L)k(L)}}|\tilde{y}(0, -i|\omega_0|)|\left(\frac{2\Delta\omega}{\Omega(L)}\right)^{1/3}\Delta\omega \sinh\left(\frac{\pi\Omega(L)}{4\Delta\omega}\right). \tag{4.14}$$

The blowup is mainly determined by the factor of hyperbolic sine.

If the spread is marginal

$$\Delta\omega \sim \sqrt{\frac{\Omega(L)}{T}} \tag{4.15}$$

so that the maximum takes place at the end of the pulse, the factor $\sinh(\pi\Omega/4\Delta\omega)$ gives $\exp(\pi\sqrt{\Omega T}/4)$, which is to be compared with the factor $\exp(\sqrt{\Omega T})$ in the absence of the frequency spread. The improvement is not enough when ΩT is large and we may need more spread. As one can see from eq(4.14), if the spread is

$$\Delta\omega \sim \Omega(L), \tag{4.16}$$

then the cumulative beam breakup is almost completely suppressed. One sees that the simple function $\Omega(s)$ defined in (3.7), especially its value at the exit of the linac, tells us not only the essential feature of the breakup but also the required frequency spread to damp it. In practice we can often tolerate some blowup and, in such a case, we should evaluate (4.14) to get the necessary and sufficient frequency spread. Normally, we shall get a value somewhere between (4.15) and (4.16).

The following simple argument given by R.L.Gluckstern (ref.4) leads to the formula for the sufficient spread (4.16). We have assumed the uniform distribution of the mode frequencies in the interval $(\omega_0 - \frac{1}{2}\Delta\omega, \omega_0 + \frac{1}{2}\Delta\omega)$. However, if we use the Lorenzian distribution

$$\frac{1}{\pi}\frac{\Delta\omega'}{(\omega - \omega_0)^2 + (\Delta\omega')^2} \qquad (-\infty < \omega < \infty),$$

the impedance becomes

$$Z(ip) = \frac{W_0}{2}\Big[\frac{1}{p + i[\omega_0] + \varepsilon + \Delta\omega'} - \frac{1}{p - i[\omega_0] + \varepsilon + \Delta\omega'}\Big],$$

which is exactly equal to (3.3) with ε replaced by $\varepsilon + \Delta\omega'$. Therefore, one can use the results in the absence of the spread. In particular, the exponent of the amplitude becomes $-(\varepsilon+\Delta\omega')t+\sqrt{\Omega(s)t}$. Thus, if we ignore ε, the maximum exponent is $\Omega/4\Delta\omega'$ at $t = \Omega/4\Delta\omega'^2$. When $\Delta\omega'/\Omega$ is of order unity, the breakup is totally suppressed. One cannot directly compare $\Delta\omega$ and $\Delta\omega'$ but this simple argument essentially gives the same results as (4.16).

Fig.9 shows the maximum amplitude X_{max} (actually, $\log_{10}\bar{X}_{max}/X_0$) as a function of the frequency spread $\Delta\omega/\Omega(L)$. The arrow indicates the location of the marginal value (4.15), where $\Delta\omega/2\pi = 3.24\,\mathrm{MHz}$. The crosses show the results of the tracking. The solid line is the maximum of $X(L,t_j)$, $(j = 1,..n_b)$ given by (4.8) and the dashed line is its approximation (4.14). The latter is valid when (4.12) holds; i.e., to the right of the arrow. One finds that X_{max} begins to decrease rapidly at the spread (4.15).

The dependence of X_{max} on the number of mode frequencies, n_f, is shown in Fig.10, where the spread is fixed to $\Delta\omega = 2\pi \times 6\,\mathrm{MHz}$ and $L = 1000\,\mathrm{m}$. The dashed line is the value given by the formula (4.14). One sees that even a small value of three gives essentially the same damping as the infinite number of frequencies. According to the parameters employed for this plot, the criterion of the required number of frequencies, (4.2), gives $n_f \gg 2$.

5. The Misalignments of the Cavities

Another source of the excitation of the deflecting mode is the misalignments of the cavities and focusing magnets. In this section, let us consider the misalignments of the cavities. The equation of motion can be written as

$$\frac{d}{ds}\Big(\gamma(s)\frac{dx_j}{ds}\Big) + \gamma(s)k(s)^2x_j(s) = \frac{eIt_b}{mc^2}\sum_{k=0}^{j} W(t_j - t_k)\Big[x_k(s) - d_c(s)\Big], \tag{5.1}$$

where, $d_c(s)$ is the displacement of cavities. The Laplace transformation (2.2) leads to

$$\frac{d}{ds}\Big(\gamma(s)\frac{dy}{ds}\Big) + \gamma(s)\Big[k(s)^2 - \frac{V(p)}{\gamma(s)}\Big]y(s,p) = S(s,p), \tag{5.2}$$

where V is defined in (2.27) and S is given by

$$S(s,p) = -\frac{V(p)}{p}d_c(s). \tag{5.3}$$

In these expressions we approximated $\hat{V}$ by V.

Let us define the Green's function $G(s,s_1)$ by

$$\frac{d}{ds}\Big(\gamma(s)\frac{dG}{ds}\Big) + \gamma(s)\Big[k(s)^2 - \frac{V(p)}{\gamma(s)}\Big]G(s,s_1) = \delta(s - s_1) \tag{5.4}$$

with the initial condition

$$G(s,s_1)=0 \qquad \text{for} \qquad s<s_1, \tag{5.5}$$

where δ is the Dirac delta function. The solution of (5.2) with the initial condition $y(0,p)=y'(0,p)=0$ can be written as

$$y(s,p)=\int_0^s G(s,s_1)S(s_1,p)ds_1. \tag{5.6}$$

As in Section 2, the WKB approximation and the assumption of the strong focusing lead to the following expression for $G(s,s_1)$;

$$G(s,s_1)=\frac{1}{\sqrt{\gamma(s)k(s)\gamma(s_1)k(s_1)}}\sin\Big[\psi(s)-\psi(s_1)-\frac{1}{2}V(p)\Big(H(s)-H(s_1)\Big)\Big], \tag{5.7}$$

where $\psi(s)$ and $H(s)$ are defined by (2.12) and (2.13).

Therefore, combining the equations (5.3), (5.6), (5.7) and (2.28), we get

$$\begin{aligned}
x(s,t)&=\frac{1}{2\pi i}\int_{-i\infty+p_c}^{+i\infty+p_c}dp\,e^{pt}\int_0^s ds_1\frac{S(s_1,p)}{\sqrt{\gamma k\gamma_1 k_1}}\sin\Big(\psi-\psi_1-\frac{1}{2}V(p)(H-H_1)\Big)\\
&=-\Re\frac{1}{2\pi}\int_{-i\infty+p_c}^{+i\infty+p_c}dp\,e^{pt}\int_0^s ds_1\frac{-V(p)d_{c1}}{p\sqrt{\gamma k\gamma_1 k_1}}e^{i(\psi-\psi_1-\frac{1}{2}V(p)(H-H_1))}\\
&=-\Re\int_0^s\frac{ds_1}{\sqrt{\gamma k\gamma_1 k_1}}e^{i(\psi-\psi_1)}\Big[2d_{c1}\frac{\partial}{\partial H}\Big]\frac{1}{2\pi i}\int_{-i\infty+p_c}^{+i\infty+p_c}e^{pt-\frac{i}{2}V(p)(H-H_1)}\frac{dp}{p}.
\end{aligned} \tag{5.8}$$

Here, the subscript 1 denotes the values at $s=s_1$.

First, consider isolated resonances. The impedance is the one given in (3.3). The integral over p appearing in (5.8) has already been introduced in Section 3, eq(3.4). We have only to replace $\tilde{y}(0,p)$ by $1/p$ and $H(s)$ by $H(s)-H(s_1)$ in the result (3.22);

$$x(s,t)=\Re\int_0^s\frac{ds_1}{\sqrt{\gamma k\gamma_1 k_1}}e^{i(\psi-\psi_1)}d_{c1}\frac{\partial}{\partial H}\frac{i}{\sqrt{2\pi[\omega_0]}}\Big(\frac{\Omega-\Omega_1}{t^3}\Big)^{1/4}e^{-i[\omega_0]t+\sqrt{(\Omega-\Omega_1)t}}. \tag{5.9}$$

Here Ω and Ω_1 denote $\Omega(s)$ and $\Omega(s_1)$ defined in (3.6). They contain H and H_1, respectively. Therefore, $\partial/\partial H$ operates on Ω. We have ignored ε, the damping factor due to the finite quality factor. We made some assumptions when we derived (3.22). One of them, namely (3.17) with $\Omega(s)$ replaced by $\Omega-\Omega_1$, is not satisfied here because the integral over s_1 in (5.9) requires the information at s_1 close to s, i.e., $\Omega(s)$ close to $\Omega(s_1)$. However, when the beam breakup is significant, we may ignore the contribution of this part because that of the part $s_1\sim 0$ is much larger. The effect of the misalignments at $s_1\sim s$ has not yet grown up at s. The partial derivative $\partial/\partial H$ gives two terms, one from the Ω in the fourth root factor and the other from that in the exponent. When $(\Omega(s)-\Omega(s_1))t\gg 1$, the former can be ignored and we get

$$x(s,t)=\Re\int_0^s\frac{ds_1}{\sqrt{\gamma k\gamma_1 k_1}}e^{i(\psi-\psi_1)}d_{c1}\sqrt{\frac{t}{\Omega-\Omega_1}}\frac{eIW_0}{mc^2}$$

$$\times \frac{i}{2\sqrt{2\pi[\omega_0]}}\Big(\frac{\Omega-\Omega_1}{t^3}\Big)^{1/4} e^{-i[\omega_0]t+\sqrt{(\Omega-\Omega_1)t}}. \tag{5.10}$$

Let us define the "normalized Courant-Snyder invariant" by

$$\epsilon(s,t) = \Big(\text{amplitude of } x(s,t)\Big)^2 \gamma(s)k(s). \tag{5.11}$$

Then the expectation value of $\epsilon(s,t)$ by random errors is given by

$$\begin{aligned} <\epsilon(s,t)>_{cav} = & \frac{1}{8\pi[\omega_0]^2}\int_0^s \frac{ds_1}{\sqrt{\gamma_1 k_1}}\int_0^s \frac{ds_2}{\sqrt{\gamma_2 k_2}} e^{i(\psi_2-\psi_1)}\Big(\frac{eIW_0}{mc^2}\Big)^2 \\ & \times <d_{c1}d_{c2}> \Big((\Omega-\Omega_1)t\Big)^{-1/4}\Big((\Omega-\Omega_2)t\Big)^{-1/4} e^{\sqrt{(\Omega-\Omega_1)t}+\sqrt{(\Omega-\Omega_2)t}} \end{aligned} \tag{5.12}$$

The subscript 2 denotes the values at $s = s_2$. We assume that there is no correlation between the misalignment errors of different cavity units. By this assumption, (5.12) can be greatly simplified as

$$<\epsilon(s,t)>_{cav} = \frac{1}{8\pi[\omega_0]^2}\int_0^s ds_1 \frac{l_c(s_1)<d_c^2(s_1)>}{\gamma_1 k_1}\Big(\frac{eIW_0}{mc_2}\Big)^2 \frac{1}{\sqrt{(\Omega-\Omega_1)t}} e^{2\sqrt{(\Omega-\Omega_1)t}}, \tag{5.13}$$

where, l_c, which can be a function of s, is the length of a cavity unit aligned independently. (Rigorously speaking, it is the center-to-center distance between ajacent cavities.) This integral states that the misalignments near the injection point are more important than those at the linac exit by the factor $\exp\sqrt{\Omega(L)T}$.

Changing the integration variable from s_1 to $\Omega_1 = \Omega(s_1)$, we can easily integrate (5.13), with the assumption that l_c and $<d_c^2>$ are independent of s;

$$\begin{aligned} <\epsilon(s,t)>_{cav} &= \frac{l_c<d_c^2>}{8\pi[\omega_0]^2}\frac{eIW_0}{mc^2}\int_0^{\Omega(s)} \frac{d\Omega_1}{\sqrt{(\Omega-\Omega_1)t}} e^{2\sqrt{(\Omega-\Omega_1)t}} \\ &= \frac{l_c<d_c^2>}{8\pi[\omega_0]^2}\frac{eIW_0}{mc^2t}\Big(e^{2\sqrt{\Omega(s)t}}-1\Big). \end{aligned}$$

The second term in the parenthesis can be ignored because of the assumption (3.17). Thus, we obtain

$$<\epsilon(s,t)>_{cav} = \frac{l_c<d_c^2>}{8\pi[\omega_0]^2}\frac{eIW_0}{mc^2t} e^{2\sqrt{\Omega(s)t}}. \tag{5.14}$$

Note the resonance behavior shown by the factor $[\omega_0]$. One sees that the breakup by misalignments is also characterized by $\exp(\sqrt{\Omega t})$ as in the case of the injection errors. It is interesting to compare these two effects. As in this section, we can define ϵ_{inj} by

$$\epsilon(s,t)_{inj} = \gamma(s)k(s)\Big(X(s,t)\Big)^2, \tag{5.15}$$

where the amplitude $X(s,t)$ is given by (3.24). For comparison we adopt the initial condition of the whole beam offset (the upper factor in the curly brackets in (3.24)). Then we have

$$\frac{<\epsilon(s,t)>_{cav}}{\epsilon(s,t)_{inj}} = \frac{<d_c^2>}{X_0^2}\frac{l_c}{\gamma_0 k_0}\frac{\sqrt{\Omega(s)t}}{H(s)} = \frac{<d_c^2>}{X_0^2}\frac{l_c}{\gamma_0 k_0}\frac{\sqrt{\Omega(s)t}}{\int_0^s ds/\gamma k}. \tag{5.16}$$

If $\gamma(s)k(s)$ is constant, then this relation states that the cavity misalignment

$$\sqrt{< d_c^2 >} \sim \sqrt{\frac{\text{number of cavity units}}{\sqrt{\Omega(L)t}}} X_0 \tag{5.17}$$

gives nearly the same blowup as the injection error X_0 does.

Fig.11 shows a comparison of (5.14) and the computer tracking, where ten machines (ten sets of Gaussian random numbers) are simulated. There, $\log_{10}\epsilon(s,t)$ (in meter radian) is plotted against the bunch index for fixed s (=2000m). The adopted parameters are $l_c = 2m$ and $\sqrt{< d_c^2 >} = 50\mu m$, and the rests are the same as given in Section 3. The crosses are the results of the tracking and the dashed line is their average. The solid line shows the formula (5.14). The agreement between the solid and dashed lines is excellent except for small t, where the assumption (3.17) fails. Also, one finds a large statistical fluctuation in the results of the tracking. This can be explained as follows. The displacement $x(s,t)$ is a sum of many Gaussian random numbers and, therefore, $\epsilon(s,t) \propto (x(s,t))^2$ obeys an exponential distribution $\exp(-\epsilon/ < \epsilon >)$. Hence, if one wants to be safe, one should multiply (5.14) by some factor, say three ($e^{-3} = 1/20$), to get a probable maximum value of $\epsilon(s,t)$.

Next, let us take into account the frequency spread. To do so, we have only to use in eq(5.8) the impedance given in (4.3). The integral over p has already been evaluated in Appendix C. The only changes here are that the factor $1/p$ in (5.8) is replaced by $i/[\omega_0]$ and the function $H(s)$ by $H(s) - H(s_1)$. Thus, we obtain

$$x(s,t) = -\Re \int_0^s \frac{ds_1}{\sqrt{\gamma k \gamma_1 k_1}} e^{i(\psi-\psi_1-[\omega_0]t)} \Big(2d_{c1}\frac{eIW_0}{mc^2}\frac{\partial}{\partial\Omega}\Big)\frac{i}{[\omega_0]}$$
$$\times \sinh\Big(\frac{\pi}{4}\frac{\Omega-\Omega_1}{\Delta\omega}\Big)\sqrt{\frac{2(\Omega-\Omega_1)}{t}}\Big[\frac{\varsigma(\Omega-\Omega_1)}{(t\Delta\omega)^2-(\Omega-\Omega_1)t}\Big]^{1/4}\mathbf{Ai}(-\varsigma(\Omega-\Omega_1)), \tag{5.18}$$

where $\varsigma(\Omega-\Omega_1)$ is given by (4.9) with $\Omega(s)$ replaced with $\Omega-\Omega_1$.

By the same assumption of the randomness as before, we can evaluate the expectation of the 'normalized Courant-Snyder invariant' as

$$< \epsilon(s,t) >_{cav} = \int_0^s \frac{ds_1}{\gamma_1 k_1}\frac{4l_c < d_c^2 >}{([\omega_0]t)^2}\Big(\frac{eIW_0}{mc^2}\Big)^2\Big[\Big(\frac{\partial f(\Omega,t)}{\partial\Omega}\Big)_{\Omega-\Omega_1}\Big]^2, \tag{5.19}$$

where

$$f(\Omega,t) = \sqrt{2\Omega t}\sinh\frac{\pi\Omega}{4\Delta\omega}\Big[\frac{\varsigma(\Omega)}{(t\Delta\omega)^2-\Omega t}\Big]^{1/4}\mathbf{Ai}(-\varsigma(\Omega)). \tag{5.20}$$

We again assume that l_c and $< d_c^2 >$ are independent of s. Then, by changing the integration variable from s_1 to $\Omega' \equiv \Omega - \Omega_1$, we obtain

$$< \epsilon(s,t) >_{cav} = \frac{4l_c < d_c^2 >}{([\omega_0]t)^2}\frac{eIW_0}{mc^2}\int_0^{\Omega(s)} d\Omega'\Big(\frac{\partial f(\Omega',t)}{\partial\Omega'}\Big)^2. \tag{5.21}$$

Consider the two cases $\varsigma(\Omega) \ll -1$ (exponential-like region) and $\varsigma(\Omega) \gg 1$ (oscillatory region). The integration for $\varsigma(\Omega)$ in the transition region can hardly be done but the two asymptotic cases above are sufficient for us. The integration path of (5.21) in the (t,Ω') plane shown in Fig.6 starts at $\Omega' = 0$, goes up vertically and ends at $\Omega' = \Omega(s)$. Hence, when the upper limit $\Omega(s)$ is in the exponential-like region, the path also goes through the oscillatory region. As one can see from Fig.7, however, its contribution is extremely small. Therefore, if $\Omega(s)$ is well inside the exponential-like region, we may use the asymptotic form of $\mathbf{Ai}(-\varsigma(\Omega'))$ for $\varsigma(\Omega') \ll -1$, (D.5). Thus, we get

$$f(\Omega',t) = \frac{(\Omega' t)^{1/4}}{2\sqrt{2\pi}} \exp\Big[\frac{1}{2}\Big(\frac{\Omega'}{\Delta\omega}\sin^{-1}\sqrt{\frac{t(\Delta\omega)^2}{\Omega'}} + \sqrt{\Omega' t - (t\Delta\omega)^2}\Big)\Big]. \qquad (5.22)$$

We have approximated $(\Omega' t - t^2\Delta\omega^2)^{1/4}$ by $(\Omega' t)^{1/4}$ and $\sinh(\pi\Omega'/4\Delta\omega)$ by $\exp(\pi\Omega'/4\Delta\omega)/2$. The derivative of the factor $(\Omega' t)^{1/4}$ with respect to Ω' is much smaller than that of the exponent and we have

$$\Big(\frac{\partial f}{\partial\Omega'}\Big)^2 = \frac{\sqrt{\Omega' t}}{32\pi(\Delta\omega)^2}\Big(\sin^{-1}\sqrt{\frac{t(\Delta\omega)^2}{\Omega'}}\Big)^2 \exp\Big[\frac{\Omega'}{\Delta\omega}\sin^{-1}\sqrt{\frac{t(\Delta\omega)^2}{\Omega'}} + \sqrt{\Omega' t - (t\Delta\omega)^2}\Big].$$

The region near the upper limit $\Omega' = \Omega(s)$ dominates in the integral. Therefore, we may expand the exponent up to the first order term in $\Omega_1 \equiv \Omega(s) - \Omega'$ and put $\Omega' = \Omega(s)$ elsewhere. Thus, we have

$$\Big(\frac{\partial f}{\partial\Omega'}\Big)^2 = \frac{\sqrt{\Omega' t}}{32\pi(\Delta\omega)^2}\Big(\sin^{-1}\sqrt{\frac{t(\Delta\omega)^2}{\Omega'}}\Big)^2 \exp\Big[\frac{\Omega'}{\Delta\omega}\sin^{-1}\sqrt{\frac{t(\Delta\omega)^2}{\Omega'}} + \sqrt{\Omega' t - (t\Delta\omega)^2}\Big]$$
$$\times \exp\Big[-\frac{\Omega_1}{\Delta\omega}\sin^{-1}\sqrt{\frac{t(\Delta\omega)^2}{\Omega}}\Big].$$

Then the integral in (5.21) can be estimated by

$$\int_0^{\Omega} d\Omega'\Big(\frac{\partial f}{\partial\Omega'}\Big)^2 = \int_0^{\Omega} d\Omega_1\Big(\frac{\partial f}{\partial\Omega'}\Big)^2 \approx \int_0^{\infty} d\Omega_1\Big(\frac{\partial f}{\partial\Omega'}\Big)^2,$$

whence, we obtain, for the exponential-like region

$$< \epsilon(s,t) >_{cav} = \frac{l_c < d_c^2 >}{8\pi(|\omega_0|t)^2}\frac{eIW_0}{mc^2}\frac{\sqrt{\Omega t}}{\Delta\omega}\sin^{-1}\sqrt{\frac{t(\Delta\omega)^2}{\Omega}}$$
$$\times \exp\Big[\frac{\Omega}{\Delta\omega}\sin^{-1}\sqrt{\frac{t(\Delta\omega)^2}{\Omega}} + \sqrt{\Omega t - (t\Delta\omega)^2}\Big] \qquad (t \ll \frac{\Omega}{(\Delta\omega)^2}). \quad (5.23)$$

This expression agrees with (5.14) in the limit of no frequency spread $\Delta\omega \to 0$.

Next, consider the case when $(t,\Omega(s))$ is in the oscillatory region. In this case, we can use the asymptotic form of $\mathbf{Ai}(-\varsigma)$ for $\varsigma \gg 1$, (D.6) and we have

$$f(\Omega',t) = \frac{(\Omega' t)^{1/4}}{\sqrt{2\pi}} \exp\frac{\pi\Omega'}{4\Delta\omega}\sin\Big[\frac{1}{2}\Big(-\frac{\Omega'}{\Delta\omega}\cosh^{-1}\sqrt{\frac{t(\Delta\omega)^2}{\Omega'}} + \sqrt{(t\Delta\omega)^2 - \Omega' t}\Big) + \frac{\pi}{4}\Big]. \quad (5.24)$$

The derivative of $(\Omega' t)^{1/4}$ can be ignored but those of the exponent and the argument of sine cannot. After differentiation and taking the square, we approximate $\sin^2$ and $\cos^2$ by their average value $1/2$ and neglect the cross term $\sin\cos$. (In practice, the number of oscillation may not be large so that this approximation is very crude.) Then, we obtain

$$\Big(\frac{\partial f}{\partial \Omega'}\Big)^2 \approx \frac{\sqrt{\Omega' t}}{16\pi(\Delta\omega)^2}\Big[\frac{\pi^2}{4} + \Big(\cosh^{-1}\sqrt{\frac{t(\Delta\omega)^2}{\Omega'}}\Big)^2\Big]\exp\frac{\pi\Omega'}{2\Delta\omega}.$$

In the same manner as in the previous case, we have

$$\int_0^{\Omega(s)} d\Omega'\Big(\frac{\partial f}{\partial \Omega'}\Big)^2 \approx \frac{\sqrt{\Omega t}}{32\Delta\omega}\Big[1 + \Big(\frac{2}{\pi}\cosh^{-1}\sqrt{\frac{t(\Delta\omega)^2}{\Omega}}\Big)^2\Big]\exp\frac{\pi\Omega}{2\Delta\omega}.$$

Thus, we obtain, for the oscillatory region,

$$< \epsilon(s,t) >_{cav} = \frac{l_c < d_c^2 >}{8(|\omega_0|t)^2}\frac{eIW_0}{mc^2}\frac{\sqrt{\Omega t}}{\Delta\omega}\Big[1 + \Big(\frac{2}{\pi}\cosh^{-1}\sqrt{\frac{t(\Delta\omega)^2}{\Omega}}\Big)^2\Big]\exp\frac{\pi\Omega}{2\Delta\omega}.$$
$$(t \gg \frac{\Omega}{(\Delta\omega)^2}). \qquad (5.25)$$

The formulae (5.23) and (5.25), which are valid in different regions, disagree at the transition point $t = \Omega/(\Delta\omega)^2$ by a factor two. This discrepancy of a factor two is beyond the accuracy of our formulae. In practice, however, this is not serious. We may use either formula up to the transition point.

As one can see from these formulae, $< \epsilon(s,t) >_{cav}$ is a rapidly increasing function of t in $t \ll \Omega/\Delta\omega^2$ and slowly decreasing in the region $t \gg \Omega/\Delta\omega^2$. As a function of s, it is monotonically increasing. Thus, the maximum takes place at the linac exit and near $t \approx \Omega/\Delta\omega^2$ (if this is within the pulse length T). The maximum value is given by (5.25), putting $t = \Omega/\Delta\omega^2$;

$$< \epsilon >_{max,cav} = \frac{l_c < d_c^2 >}{8[\omega_0]^2}\frac{eIW_0}{mc^2}\frac{\Omega(L)}{(\Delta\omega)^2}\exp\frac{\pi\Omega(L)}{2\Delta\omega} \qquad (T > \frac{\Omega(L)}{(\Delta\omega)^2}). \qquad (5.26)$$

If $T < \Omega(L)/\Delta\omega^2$, the maximum is at the end of the pulse and is given by (5.23) with $s = L$ and $t = T$. In the former case, i.e., when the frequency spread $\Delta\omega$ is large enough to satisfy (4.12), one finds that the frequency spread can cause damping of the beam breakup due to the cavity misalignments as it can in the case of the injection errors. The formulae (5.23) and (5.25) are compared with the tracking in Fig.12. The frequency spread of 6 MHz is adopted. Other parameters and the captions are the same as in Fig.11. The two solid lines represent (5.23) and (5.25). This time, the agreement is not very good because of the crude approximations employed to get the analytic formulae. An oscillatory behavior is seen in the tracking but it is not expressed by the analytic formulae because we have put $\sin^2 \sim \cos^2 \sim 1/2$ and ignored the cross term. Moreover, our tracking parameters are not

far from the transition region. Nevertheless, our formulae still describe the average behavior quite well.

6. The Misalignments of the Focusing Elements.

The misalignments of the focusing magnets can also enhance the cumulative beam breakup. The effects of other dipole fields on the axis such as the steering magnets can be treated in the same manner. The equation of motion can be written as

$$\frac{d}{ds}\left(\gamma(s)\frac{dx_j}{ds}\right) + \gamma(s)k(s)^2 x_j(s) = \frac{eIt_b}{mc^2}\sum_{k=0}^{j} W(t_j - t_k)x_k(s) + \gamma(s)g(s). \tag{6.1}$$

Here, $g(s)$ is the orbital curvature due to the misalignments of quadrupole magnets and other dipole fields. By the Laplace transformation we get the same equation as (5.2) but, now S is given by

$$S(s,p) = \frac{\gamma(s)}{p}g(s). \tag{6.2}$$

Therefore, instead of (5.8) we get

$$x(s,t) = -\Re\int_0^s \frac{ds_1}{\sqrt{\gamma k \gamma_1 k_1}} e^{i(\psi-\psi_1)}\gamma_1 g_1 \frac{1}{2\pi}\int_{-i\infty+p_c}^{+i\infty+p_c} e^{pt-\frac{i}{2}V(p)(H-H_1)}\frac{dp}{p}. \tag{6.3}$$

The subscript 1 denotes the values at $s = s_1$, as in the previous section. This is valid for arbitrary $g(s)$ but here we shall consider random errors only. We do not study the problem of the orbit correction. (This can also be taken into account by $g(s)$ but it's not random.)

First, consider isolated resonances. The integral over p in (6.3) can be carried out with the result

$$x(s,t) = -\Re\int_0^s \frac{ds_1}{\sqrt{\gamma k \gamma_1 k_1}} e^{i(\psi-\psi_1)}\frac{\gamma_1 g_1}{2\sqrt{2\pi}[\omega_0]}\left(\frac{\Omega-\Omega_1}{t^3}\right)^{1/4} e^{-i[\omega_0]t+\sqrt{(\Omega-\Omega_1)t}}. \tag{6.4}$$

The expectation value of $\epsilon(s,t)$ by random errors is given by

$$\begin{aligned} <\epsilon(s,t)>_q = & \frac{1}{8\pi[\omega_0]^2}\int_0^s \frac{ds_1}{\sqrt{\gamma_1 k_1}}\int_0^s \frac{ds_2}{\sqrt{\gamma_2 k_2}} e^{i(\psi_2-\psi_1)} <\gamma_1 g_1 \gamma_2 g_2> \\ & \times \left(\frac{\Omega-\Omega_1}{t^3}\right)^{1/4}\left(\frac{\Omega-\Omega_2}{t^3}\right)^{1/4} e^{\sqrt{(\Omega-\Omega_1)t}+\sqrt{(\Omega-\Omega_2)t}} \end{aligned} \tag{6.5}$$

Assuming no correlation between the misalignment errors of different quadupole magnets, we get

$$<\epsilon(s,t)>_q = \frac{1}{8\pi[\omega_0]^2}\int_0^s ds_1 \frac{n_q(s_1)\gamma_1}{k_1} <\theta_q^2> \sqrt{\frac{\Omega-\Omega_1}{t^3}} e^{2\sqrt{(\Omega-\Omega_1)t}}, \tag{6.6}$$

where n_q is the number of the quadrupole magnets in unit length and θ_q is the kick angle by a misaligned magnet. If the focusing structure is FODO (one quad in a half cell) and the phase advance per cell is μ_{cell}, we have

$$\theta_q \approx 4kd_q\frac{1}{\mu_{cell}}\sin\frac{\mu_{cell}}{2} \approx 2kd_q \qquad \text{and} \qquad n_q \approx \frac{2k}{\mu_{cell}}, \tag{6.7}$$

where d_q is the displacement of the quadrupole magnets. Then, eq(6.6) can be written as

$$< \epsilon(s,t) >_q = \frac{1}{\pi([\omega_0]t)^2} \int_0^s ds_1 < d_q^2 > \frac{k_1^2 \gamma_1}{\mu_{cell}} \sqrt{(\Omega - \Omega_1)t}\, e^{2\sqrt{(\Omega-\Omega_1)t}}. \tag{6.8}$$

For an arbitrarily given $k(s)$, this expression must be numerically integrated, but in order to have a rough estimate we assume that the focussing strength varies as $k \propto \gamma^{-\alpha}$; i.e.,

$$k(s) = k_0 \Big(\frac{\gamma(s)}{\gamma_0}\Big)^{-\alpha} \qquad (0 \le \alpha \le 1). \tag{6.9}$$

The constant optics and the constant field gradient are given by $\alpha = 0$ and 1, respectively. The actual design will be somewhere in between. We shall call an optic with small α (close to zero) 'hard' optic and that with large α (close to unity) 'soft'. The hard optic is the one where the focusing is kept strong up to high energy.

Further, we assume that μ_{cell}, $< d_q^2 >$ and the acceleration rate $d\gamma/ds$ are constant. Then, after some manipulation, we get

$$\begin{aligned} < \epsilon(s,t) >_q &= \frac{< d_q^2 >}{\pi([\omega_0]t)^2} \frac{(\gamma_0 k_0)^2}{\mu_{cell}(d\gamma/ds)} \\ &\quad \times \kappa_1(s) \int_0^1 d\xi (1 + \alpha\kappa_1(s)\xi)^{(2-3\alpha)/\alpha} \sqrt{\Omega(s)t(1-\xi)}\, e^{2\sqrt{\Omega(s)t(1-\xi)}} \\ &= \frac{< d_q^2 >}{\pi([\omega_0]t)^2} \frac{(\gamma_0 k_0)^2}{\mu_{cell}(d\gamma/ds)} e^{2\sqrt{\Omega(s)t}} \kappa_1(s) \Big[1 + (3\alpha - 2)\frac{\kappa_1}{\sqrt{\Omega t}}\Big]^{-1} \end{aligned} \tag{6.10}$$

with

$$\kappa_1(s) = \int_{\gamma_0}^{\gamma(s)} \Big(\frac{\gamma}{\gamma_0}\Big)^{\alpha-1} \frac{d\gamma}{\gamma_0} = \left\{ \begin{array}{ll} \frac{1}{\alpha}\Big[(\gamma/\gamma_0)^\alpha - 1\Big] & (0 < \alpha \le 1) \\ \log(\gamma/\gamma_0) & (\alpha = 0) \end{array} \right\} \tag{6.11}$$

where we have assumed (3.17). The last factor in the square brackets in (6.10) comes from a crude approximation $\kappa_1 \ll \sqrt{\Omega(s)t}$, but it does not give a big error even for $\kappa_1 \sim \sqrt{\Omega(s)t}$. For a large value of $\kappa_1/\sqrt{\Omega(s)t}$, one has to integrate (6.8) numerically. However, one must be careful if the last factor is negative or has a very small positive value, which can happen when $\alpha < 2/3$. In such a case the major contribution in (6.8) does not come from $s_1 \sim 0$ but some large value of s_1. Then, we cannot use (6.4), which is valid only for large $\Omega - \Omega_1$, and our formula (6.10) fails. Physically speaking, the situation is as follows. When the optic is hard, the kick angle by a given misalignment d_q is nearly the same in the low and high energy part of the linac but the high energy part contributes to $< \epsilon >_q$ more than the low energy part because of the adiabatic damping factor. Thus, (6.10) is valid when

$$1 \gtrsim (3\alpha - 2)\frac{\kappa_1(s)}{\sqrt{\Omega(s)t}} \gg -1. \tag{6.12}$$

In the absence of the wake or, equivalently, in the limit of low current, the misalignments of quads give rise to the orbit distortion

$$x_{cod}(s) = -\Re \int_0^s \frac{ds_1}{\sqrt{\gamma k \gamma_1 k_1}} e^{i(\psi - \psi_1)} i\gamma_1 g(s_1). \tag{6.13}$$

The same assumptions as before give

$$< \epsilon(s) >_{q,cod} = \int_0^s \frac{n_q \gamma_1}{k_1} < \theta_q^2 > ds_1 = \frac{8 < d_q^2 >}{\mu_{cell}} \int_0^s k_1^2 \gamma_1 ds_1$$
$$= \frac{8 < d_q^2 > (\gamma_0 k_0)^2}{\mu_{cell}(d\gamma/ds)} \kappa_2(s) \tag{6.14}$$

with

$$\kappa_2(s) = \frac{1}{2-2\alpha}\Big[\Big(\frac{\gamma}{\gamma_0}\Big)^{2-2\alpha} - 1\Big]. \tag{6.15}$$

Comparing (6.10) and (6.14), we have

$$\frac{< \epsilon(s,t) >_q}{< \epsilon(s,t) >_{q,cod}} = \frac{\exp\Big(2\sqrt{\Omega(s)t}\Big)}{8\pi(|\omega_0|t)^2} \frac{\kappa_1(s)}{\kappa_2(s)}, \tag{6.16}$$

where we have ignored the correction factor in (6.10). When the optic is hard, the high energy part contributes to $< \epsilon >_{q,cod}$ very much and, therefore, the ratio κ_1/κ_2 becomes small.

Now, turn to the problem of the frequency spread. Instead of (6.4), we have

$$x(s,t) = \Re \int_0^s \frac{ds_1}{\sqrt{\gamma k \gamma_1 k_1}} e^{i(\psi - \psi_1 - |\omega_0|t)} \frac{\gamma_1 g_1}{|\omega_0|t} f(\Omega - \Omega_1, t), \tag{6.17}$$

where f is defined in (5.20). This leads to the expectation of the 'normalized Courant-Snyder invariant'

$$< \epsilon(s,t) >_q = \frac{8}{(|\omega_0|t)^2} \int_0^s ds_1 \Big[\frac{k^2 \gamma < d_q^2 >}{\mu_{cell}}\Big]_{s=s_1} \Big[f(\Omega - \Omega_1, t)\Big]^2. \tag{6.18}$$

Changing the integration variable from s_1 to Ω_1, by using (3.6), and applying the explicit form of the optics (6.9), we get

$$< \epsilon(s,t) >_q = \frac{8 < d_q^2 > k_0^3 \gamma_0^2}{(|\omega_0|t)^2 \mu_{cell}} \Big(\frac{eIW_0}{mc^2}\Big)^{-1} \int_0^{\Omega(s)} d\Omega_1 \Big(\frac{\gamma_1}{\gamma_0}\Big)^{2-3\alpha} \Big[f(\Omega - \Omega_1, t)\Big]^2. \tag{6.19}$$

When $(t, \Omega(s))$ is in the exponential-like region, we may use the asymptotic form of f, (5.22). The same method which was employed in order to derive (5.23) gives

$$< \epsilon(s,t) >_q = \frac{< d_q^2 > k_0^2 \gamma_0^2}{\pi(|\omega_0|t)^2 \mu_{cell}(d\gamma/ds)} \exp\Big[\frac{\Omega(s)}{\Delta\omega} \sin^{-1} \sqrt{\frac{t(\Delta\omega)^2}{\Omega(s)}} + \sqrt{\Omega(s)t - (t\Delta\omega)^2}\Big]$$
$$\times \kappa_1(s) \Big[\sqrt{\frac{\Omega(s)}{t(\Delta\omega)^2}} \sin^{-1} \sqrt{\frac{t(\Delta\omega)^2}{\Omega(s)}} + (3\alpha - 2)\frac{\kappa_1(s)}{\sqrt{\Omega(s)t}}\Big]^{-1} \qquad (t < \frac{\Omega(s)}{(\Delta\omega)^2}). \tag{6.20}$$

This coincides with (6.10) in the limit of $\Delta\omega \to 0$. The last factor must be treated in the same way as before; namely, if it is negative, this formula fails.

Similarly, when $(t, \Omega(s))$ is in the oscillatory region, we get, by using (5.24),

$$< \epsilon(s,t) >_q = \frac{2 < d_q^2 > k_0^2 \gamma_0^2}{\pi(|\omega_0|t)^2 \mu_{cell}(d\gamma/ds)} \exp \frac{\pi\Omega(s)}{2\Delta\omega}$$

$$\times \kappa_1(s)\Big[\frac{\pi}{2}\sqrt{\frac{\Omega(s)}{t(\Delta\omega)^2}}+(3\alpha-2)\frac{\kappa_1(s)}{\sqrt{\Omega(s)t}}\Big]^{-1} \qquad (t>\frac{\Omega(s)}{(\Delta\omega)^2}), \qquad (6.21)$$

where we have used the approximation $\sin^2 \sim 1/2$ in $f^2(\Omega-\Omega_1,t)$. Again, one finds the discrepancy between (6.20) and (6.21) by a factor two at $t=\Omega/\Delta\omega^2$ but it is not important. Comparing (6.20) and (6.21), one finds that the maximum takes place around $t\sim\Omega/\Delta\omega^2$, if this is within the given bunch length. The maximum value is

$$< \epsilon(s,t) >_q = \frac{2<d_q^2>k_0^2\gamma_0^2}{\pi[\omega_0]^2\mu_{cell}(d\gamma/ds)}\frac{(\Delta\omega)^4}{\Omega(L)^2}\exp\frac{\pi\Omega(L)}{2\Delta\omega}$$
$$\times\kappa_1(L)\Big[\frac{\pi}{2}+(3\alpha-2)\frac{\kappa_1(s)\Delta\omega}{\Omega(L)}\Big]^{-1} \qquad (T>\frac{\Omega(L)}{(\Delta\omega)^2}). \qquad (6.22)$$

If the spread is small so that (4.12) is not satisfied, the maximum occurs at the end of the pulse and its value is given (6.20) with $t=T$ and $s=L$. One again finds the same factor $\exp(\pi\Omega(L)/2\Delta\omega)$ under the sufficient frequency spread as in the case of the injection errors, (4.14), and of the cavity misalignments, (5.26).

7. Summary

We have investigated the problem of cumulative beam breakup in a way suitable for large-scale linacs and have derived several formulae. The solutions to the problem of the initial beam offset were given in Section 3 and 4. If there is only one deflecting mode, the behavior of the beam is described by eq(3.22) with the initial condition (2.16) or (2.17). Even if there are several modes, the solution is a superposition of (3.22), provided the mode frequencies are well separated from each other so as to satisfy (3.12) with (3.14).

When several mode frequencies are concentrated within a narrow frequency band $\Delta\omega$, the beam behavior is represented by (4.7). If $\Delta\omega$ is large enough to satisfy (4.12), this frequency spread can cause considerable damping of the breakup phenomena. The maximum amplitude in such a case is given by (4.14).

For the problem of the random misalignments, we have expressed the results in terms of the expectation of the 'normalized Courant-Snyder invariant' defined in (5.11). The misalignments of the cavities are discussed in Section 5. If only one mode is responsible, the solution is given by (5.14). The effect of the frequency spread is expressed by (5.23) and (5.25). If the frequency spread is so large that eq(4.12) is fulfilled, the maximum Courant-Snyder invariant shows damping, as expressed by (5.26).

Random misalignments of the quadrupole magnets are treated in Section 7. The final formula for a single mode case is given in (6.10) and those for the frequency spread in (6.20) and (6.21). The maximum in the presence of the spread is given by (6.22). These formulae are valid when (6.12) is satisfied.

In all cases above, we found that the function $\Omega(s)$ defined by (3.6), in particular its value at the exit of the linac $\Omega(L)$, plays an essential role. The amplitude in the absence of

frequency spread is characterized by the factor $\exp(\sqrt{\Omega t})$, t being the time delay from the head of the pulse. The critical frequency spread above which the damping is significant can also be expressed by $\Omega(s)$ as shown in (4.12). Above this critical spread, the amplitude blowup is characterized by the factor $\exp(\pi\Omega(L)/4\Delta\omega)$. It turned out that frequency spread is a very poweful cure for cumulative beam breakup, although it does not work for single-bunch blowup.

References

1) R.Helm and G.Loew, *Beam Breakup*, Chapter B in *Linear Accelerators* (eds. P.M.-Lapostolle and A.L.Septier), North Holland Book Co., Amsterdam 1970.

2) V.K.Neil, L.S.Hall and R.K.Cooper, *Further Theoretical Studies of the Beam Beakup Instability* , Part.Acc., 213,**9**,(1979).

3) R.L.Gluckstern, R.K.Cooper and P.J.Channell, *Cumulative Beam Breakup in RF Linacs* , Part.Acc.,125,**16**,(1985).

4) R.L.Gluckstern, private communication.

5) A.W.Chao, B.Richter and C.Yao, *Beam Emittance Growth Caused by Transverse Deflecting Fields in a Linear Accelerator* , Nucl.Instr.Meth.,1,**178**,(1980).

6) *Handbook of Mathematical Functions with Formulas, Graphs and Mathematical Tables* , eds. M.Abramowitz and I.A.Stegun, National Bereau of Standards, Applied Mathematics Series 55.

Acknowledgement

The author would like to thank Professor Gluckstern and Dr. Cooper for their helpful suggestions and careful reading of the manuscript. He is also grateful to G.A.Voss and T.Weiland for offering him an opportunity to work at DESY.

Appendix A. Single Bunch Blowup

In this appendix we apply the same method as in the text to the problem of the transverse blowup of a single bunch in order to demonstrate the usefulness of the method. The result has already been given by A.Chao, B.Richter and C.Yao (ref.5).

In the case of the single bunch, we don't need the subtle interpretation of $[\omega_0]$ and we can start with the equation of motion of the continuous beam;

$$\frac{d}{ds}\left(\gamma(s)\frac{dx}{ds}\right) + \gamma(s)k(s)^2x(s,t) = \frac{eI}{mc^2}\int_0^t W(t-t')x(s,t')dt', \qquad \text{(A.1)}$$

where $x(s,t)$ is the transverse displacement of the portion of the bunch specified by t and the location s. We define $t = 0$ at the head of the bunch. Eq(A.1) is valid for uniform

charge distribution in the bunch with the constant current I. In contrast to the case of the multi-bunch we can define the Laplace transform of $x(s,t)$ in the continuos form;

$$y(s,p) = \int_0^\infty dt\, e^{-pt} x(s,t) \qquad (\Re p > p_c). \tag{A.2}$$

The inverse transformation is

$$x(s,t) = \frac{1}{2\pi i} \int_{-i\infty+p_c}^{+i\infty+p_c} dp\, e^{pt} y(s,p). \tag{A.3}$$

We get the same differential equation of $y(s,p)$ as (2.7) with $\hat{V}$ replaced with V in (2.27), defining the impedance $Z(ip)$ by the usual expression (2.23). The initial condition of $y(s,p)$ is

$$y(0,p) = \int_0^\infty dt\, e^{-pt} x(0,t), \qquad y'(0,p) = \int_0^\infty dt\, e^{-pt} x'(0,t), \tag{A.4}$$

instead of (2.15). The solution is given by (2.28);

$$x(s,t) = \sqrt{\frac{\gamma_0 k_0}{\gamma(s)k(s)}}\, \Re \frac{e^{i\psi(s)}}{2\pi i} \int_{-i\infty+p_c}^{+i\infty+p_c} \tilde{y}(0,p) e^{\varphi(p)} \tag{A.5}$$

with $\varphi(p)$ defined by (2.26) and (2.27).

We assume that the bunch is so short that the wake potential $W(t)$ can be approximated within the bunch by

$$W(t) = W_1 t \qquad (t > 0, W_1 > 0) \tag{A.6}$$

which gives

$$Z(ip) = -i\frac{W_1}{p^2}. \tag{A.7}$$

Hence, $\varphi(p)$ defined in (2.26) is

$$\varphi(p) = pt - i\frac{eIH(s)W_1}{2mc^2}\frac{1}{p^2} = pt - i\frac{C}{2p^2}, \tag{A.8}$$

where

$$C = \frac{eIH(s)W_1}{mc^2}. \tag{A.9}$$

There are three saddle points;

$$p_1 = \left(\frac{C}{t}\right)^{1/3} e^{-\pi i/6}, \quad p_2 = \left(\frac{C}{t}\right)^{1/3} e^{+\pi i/2}, \quad p_3 = \left(\frac{C}{t}\right)^{1/3} e^{-2\pi i/3}, \tag{A.10}$$

of which p_1 dominates at large t. We assume that the whole bunch is offset by X_0 at the injection. This leads to the initial condition

$$y(0,p) = \frac{X_0}{p}. \tag{A.11}$$

Since

$$\varphi(p_1) = \frac{2}{3}C^{1/3}t^{2/3}e^{-\pi i/6} \quad \text{and} \quad \varphi''(p_1) = 3t^{4/3}C^{-1/3}e^{\pi i/6}, \tag{A.12}$$

we get

$$\begin{aligned}\frac{1}{2\pi i}\int_{-i\infty+p_c}^{+i\infty+p_c} y(0,p)e^{\varphi(p)}dp &\approx \frac{1}{2\pi i}\int_{-i\infty}^{+i\infty} y(0,p_1)\exp\Big[\varphi(p_1)+\frac{1}{2}\varphi''(p_1)(p-p_1)^2\Big]dp \\ &= \frac{X_0}{\sqrt{6\pi}}t^{-1/3}C^{-1/6}\exp(\frac{3}{2}C^{1/3}t^{2/3}e^{-\pi i/6}+\frac{\pi i}{12}),\end{aligned} \tag{A.13}$$

where we approximated $y(0,p)$ by $y(0,p_1)$. Then we obtain from (A.5)

$$x(s,t) = \sqrt{\frac{\gamma_0 k_0}{\gamma(s)k(s)}}\frac{X_0}{\sqrt{6\pi}}\eta^{-1/6}\exp(\frac{\sqrt{3}}{4}\eta^{1/3})\cos\Big(\psi(s)+\frac{\pi}{12}-\frac{3}{4}\eta^{1/3}\Big) \tag{A.14}$$

where

$$\eta(s,t) = Ct^2 = \frac{eIH(s)W_1}{mc^2}t^2. \tag{A.15}$$

This result exactly coincides with that of ref.5.

The present method is very flexible and can be applied to various cases. For example, one can estimate the effect of the wake

$$W(t) = W_1 t(1+w_2 t), \tag{A.16}$$

if w_2 term is not as large as the first term in the given bunch length. Instead of (A.14) we obtain, up to the order of w_2^2,

$$\begin{aligned}x(s,t) =& \sqrt{\frac{\gamma_0 k_0}{\gamma k}}\frac{X_0}{\sqrt{6\pi}}\eta^{-1/6}\exp\Big[\frac{\sqrt{3}}{4}\eta^{1/3}+(1-\frac{\sqrt{3}}{2}\eta^{-1/3})w_2 t-(\frac{3\sqrt{3}}{4}\eta^{-1/3}+\frac{7}{2}\eta^{-2/3})w_2^2t^2\Big] \\ &\times\cos\Big[\psi(s)+\frac{\pi}{12}-\frac{3}{4}\eta^{1/3}-\frac{1}{2}\eta^{-1/3}w_2 t-(\frac{3}{4}\eta^{-1/3}+\frac{7\sqrt{3}}{4}\eta^{-2/3})w_2^2t^2\Big]\end{aligned} \tag{A.17}$$

This may be useful for the short-wavelength linac for future linear colliders with a relatively long bunch length to relax the problem of the beamstrahlung. One disadvantage of the present method may be that it cannot handle an arbitrary charge distribution in the bunch.

Appendix B. Steady State

As can be seen in (3.22), our solution damps away in the limit $t \to \infty$ due to the factor $e^{-\varepsilon t}$ coming from the quality factor of the mode. However, if the whole beam is offset at the injection, this result is obviously incorrect. This is because we have ignored the possible singularity of $\tilde{y}(0,p)$ in the integral of (3.8). For such a limiting value of t, all the saddle points in Fig.1. are to the left of the imaginary axis and their contribution dies away as $t \to \infty$. On the other hand $\tilde{y}(0,p)$ has poles, in general, on the imaginary axis. Their contribution

is finite at $t \to \infty$. We are not much interested in this case because the pulse length longer than the filling time does not lead to the saving of the electricity. However, it can still be intersting in the case of CW linear colliders using superconducting cavities.

For example, if the beam offset at the injection is modulated as

$$x_j(0) = X_0 \cos(|\omega_{in}|t_j + \phi_{in}), \qquad x'_j(0) = X'_0 \sin(|\omega_{in}|t_j + \phi'_{in}), \tag{B.1}$$

their Laplace transform $\tilde{y}(0,p)$, defined in (2.15) and (2.22), is

$$\tilde{y}(0,p) = \sum_{\pm} \frac{C_{\pm} t_b}{1 - e^{-(p \mp i|\omega_{in}|)t_b}}. \tag{B.2}$$

with

$$C_{\pm} = \frac{1}{2}\left(X_0 e^{\pm i\phi_{in}} \mp \frac{X'_0}{k_0} e^{\pm i\phi'_{in}}\right). \tag{B.3}$$

The poles of $\tilde{y}(0,p)$ are located at $p = \pm i|\omega_{in}| + in\omega_b$, n being any integer. In practice, we may ignore the terms with $n \neq 0$ and put

$$\tilde{y}(0,p) = \sum_{\pm} \frac{C_{\pm}}{p \mp i|\omega_{in}|}. \tag{B.4}$$

(When $|\omega_{in}|/\omega_b$ is near $1/2$, i.e., near the midway between two resonances, this approximation gives wrong results by about factor two. If one needs more accurate values, one should take up to $n = 1$ or -1.) The contribution of these poles can easily be evaluated as

$$\frac{1}{2\pi i}\int_{-i\infty+p_c}^{+i\infty+p_c} \tilde{y}(0,p)e^{\varphi(p)}dp = \sum_{\pm} C_{\pm} e^{\varphi(\pm i|\omega_{in}|)} \tag{B.5}$$

$$= \sum_{\pm} C_{\pm} \exp\left[\pm i|\omega_{in}|t - \frac{i}{2}\frac{\Omega(s)|\omega_0|}{(\varepsilon \pm i|\omega_{in}|)^2 + |\omega_0|^2}\right], \tag{B.6}$$

where we have used (3.9). Let us ignore the contribution of the deflecting mode to the phase of the oscillation and retain the contribution to the amplitude only. Then (B.6) becomes

$$\sum_{\pm} C_{\pm} \exp\left[\pm i|\omega_{in}|t \mp \frac{\Omega(s)|\omega_0||\omega_{in}|\varepsilon}{(\varepsilon^2 - (|\omega_{in}| - |\omega_0|)^2)(\varepsilon^2 + (|\omega_{in}| + |\omega_0|)^2)}\right].$$

Therefore, at large s, the term C_- (C_+) blows up if $|\omega_0||\omega_{in}| > 0$ (< 0). Thus, $x(s,t)$ in (2.28) is given by

$$x(s,t) = \sqrt{\frac{\gamma_0 k_0}{\gamma k}}\Re\left(C_{\mp} e^{i(\psi(s) \mp |\omega_{in}|t)}\right) \exp\left[\frac{\Omega(s)\varepsilon|\omega_0||\omega_{in}|}{(\varepsilon^2 + (|\omega_{in}| - |\omega_0|)^2)(\varepsilon^2 + (|\omega_{in}| + |\omega_0|)^2)}\right], \tag{B.7}$$

where the upper (lower) sign is to be taken for $|\omega_0||\omega_{in}| > 0$ (< 0).

It is easy to find the steady state at $t \to \infty$ even in the presence of the frequency spread. We have only to use the impedance (4.3) for $\varphi(\pm i[\omega_{in}])$ in (B.5). We have

$$x(s,t) = \sqrt{\frac{\gamma_0 k_0}{\gamma k}}\Re\sum_{\pm} C_{\pm}\exp\Big\{i\psi(s) \pm i[\omega_{in}]t - \frac{i\Omega(s)}{4\Delta\omega} \\ \times \Big[\log\frac{\pm i[\omega_{in}] + \varepsilon + i([\omega_0] + \frac{1}{2}\Delta\omega)}{\pm i[\omega_{in}] + \varepsilon + i([\omega_0] - \frac{1}{2}\Delta\omega)} + \log\frac{\pm i[\omega_{in}] + \varepsilon - i([\omega_0] + \frac{1}{2}\Delta\omega)}{\pm i[\omega_{in}] + \varepsilon - i([\omega_0] - \frac{1}{2}\Delta\omega)}\Big]\Big\} \quad \text{(B.8)}$$

As in the case of no spread, C_- (C_+) dominates when $[\omega_0][\omega_{in}] > 0$ (< 0). Thus we get

$$x(s,t) = \sqrt{\frac{\gamma_0 k_0}{\gamma k}}\Re\Big(C_{\mp}e^{i(\psi(s)\mp[\omega_{in}]t)}\Big) \\ \times \exp\Big\{\frac{\Omega(s)}{4\Delta\omega}\tan^{-1}\frac{4\Delta\omega\varepsilon[\omega_0][\omega_{in}]}{\Big(\varepsilon^2 + ([\omega_0] + [\omega_{in}])^2 - \frac{1}{4}\Delta\omega^2\Big)\Big(\varepsilon^2 + ([\omega_0] - [\omega_{in}])^2 - \frac{1}{4}\Delta\omega^2\Big)}\Big\} \quad \text{(B.9)}$$

The sign convention is the same as in (B.7). We have ignored the contribution of the wake to the oscillation phase. It is easy to see that this agrees with (B.7) in the limit of $\Delta\omega \to 0$. This expression is valid when ω_{in} does not resonate with the cavity; i.e., $[\omega_{in}]$ is not in the frequency band $([\omega_0] - \Delta\omega/2, [\omega_0] + \Delta\omega/2)$. (Otherwise, the pole of $\tilde{y}(0,p)$ is close to the branch cut of $\varphi(p)$ and we cannot simply extract the contribution of the pole.)

Appendix C. Integration of (4.5)

In this appendix we evaluate the integral $F(s,t)$ defined in (4.5);

$$F(s,t) = \frac{1}{2\pi i}\int_{-i\infty+p_c}^{+i\infty+p_c}\exp\Big[pt + \frac{\Omega}{4i\Delta\omega}\log\frac{p + \varepsilon + i([\omega_0] + \frac{1}{2}\Delta\omega)}{p + \varepsilon + i([\omega_0] - \frac{1}{2}\Delta\omega)}\Big]dp, \quad \text{(C.1)}$$

where the integration path is to the right of all the singularities of the integrand. Rewriting $p'_c + \varepsilon + i[\omega_0]$ by p'_c, we can simplify this expression as

$$F(s,t) = \frac{e^{-\varepsilon t - i[\omega_0]t}}{2\pi i}\int_{-i\infty+p'_c}^{+i\infty+p'_c}\exp\Big[p't + \frac{\Omega}{4i\Delta\omega}\log\frac{p' + \frac{i}{2}\Delta\omega}{p' - \frac{i}{2}\Delta\omega}\Big]dp'. \quad \text{(C.2)}$$

There is a branch cut on the imaginary axis between $-\frac{i}{2}\Delta\omega$ and $\frac{i}{2}\Delta\omega$ and the integration path runs on the right of the imaginary axis. Since the integrand is exponentially small for $\Re p' \to -\infty$, we can close the path by adding the left hemi-circle of infinite radius, as is shown in Fig.13 by the dashed line. It can be deformed so as to enclose the branch cut as shown by the solid line. The imaginary part of the logarithm is π ($-\pi$) on the right (left) of the imaginary axis. Hence, we get

$$F(s,t) = \frac{e^{-\varepsilon t - i[\omega_0]t}}{2\pi i}\int_{-i\Delta\omega/2}^{+i\Delta\omega/2}\exp\Big[p't + \frac{\Omega}{4i\Delta\omega}\log\Big|\frac{p' + \frac{i}{2}\Delta\omega}{p' - \frac{i}{2}\Delta\omega}\Big|\Big]\Big(e^{\frac{\pi\Omega}{4\Delta\omega}} - e^{-\frac{\pi\Omega}{4\Delta\omega}}\Big)dp' \\ = \frac{e^{-\varepsilon t - i[\omega_0]t}}{2\pi}\Delta\omega\sinh\Big(\frac{\pi\Omega}{4\Delta\omega}\Big)\int_{-1}^{1}e^{-i\Phi(z)}dz, \quad \text{(C.3)}$$

with

$$\Phi(z) = \frac{a}{4}\log\frac{1+z}{1-z} - \frac{b}{2}z \tag{C.4}$$

and

$$a = \frac{\Omega}{\Delta\omega}, \qquad b = t\Delta\omega \qquad (a, b > 0).$$

We shall not employ the saddle point method here because of the reason to be explained later, but it is still suggestive. The saddle points, i.e., zeroes of $\Phi'(z)$, are given by

$$z_\pm = \pm\sqrt{1-\frac{a}{b}}. \tag{C.5}$$

When $a/b < 1$, they are on the real axis and become closer to each other as a/b increases. They coalesce when $a/b = 1$ and split again to the positive and negative imaginary axis for $a/b > 1$. The simplest function which shows a similar behavoir is

$$\Psi(\xi) = \frac{1}{3}\xi^3 - \varsigma\xi - c, \tag{C.6}$$

where ς and c are constants to be determined later. The zeroes of $\Psi'(\xi)$ are $\xi_\pm = \pm\sqrt{\varsigma}$, which are real (pure imaginary) for $\varsigma > 0$ ($\varsigma < 0$). Let us change the integration variable from z to ξ, defining the latter by $\Phi(z) = \Psi(\xi)$. We fix ς and c so that $\xi = \xi_\pm$ when $z = z_\pm$. This can be achieved by $c = 0$ and

$$\frac{2}{3}\varsigma^{\frac{3}{2}} = -\frac{a}{4}\log\frac{1+\sqrt{1-a/b}}{1-\sqrt{1-a/b}} + \frac{1}{2}b\sqrt{1-\frac{a}{b}}, \tag{C.7}$$

or, more definitely,

$$\begin{aligned}\varsigma &= +\left[\frac{3}{4}\left(-a\cosh^{-1}\sqrt{\frac{b}{a}} + \sqrt{b^2-ab}\right)\right]^{2/3} \qquad (a < b)\\ &= -\left[\frac{3}{4}\left(+a\cos^{-1}\sqrt{\frac{b}{a}} - \sqrt{ab-b^2}\right)\right]^{2/3} \qquad (a > b).\end{aligned} \tag{C.8}$$

As a function of a and b, ς satisfies

$$\begin{aligned}\frac{\partial\varsigma}{\partial a} &= -\frac{1}{2\sqrt{\varsigma}}\cosh^{-1}\sqrt{\frac{b}{a}} \qquad (a < b)\\ &= -\frac{1}{2\sqrt{\varsigma}}\cos^{-1}\sqrt{\frac{b}{a}} \qquad (a > b)\end{aligned} \tag{C.9}$$

and

$$\frac{\partial\varsigma}{\partial b} = \frac{1}{2}\sqrt{\frac{b-a}{\varsigma b}}. \tag{C.10}$$

These expressions look singular but in truth ς is smooth at $a = b$.

Now, the relation $\Phi(z) = \Psi(\xi)$, or

$$\frac{a}{4}\log\frac{1+z}{1-z} - \frac{bz}{2} = \frac{\xi^3}{3} - \varsigma\xi \tag{C.11}$$

determines ξ definitely. The points $z = 0, z_\pm, \pm 1$ correspond to $\xi = 0, \xi_\pm, \pm\infty$, respectively. The function $z(\xi)$ is smooth in $-\infty < \xi < \infty$ and monotonically increasing.

Thus, the integral in (C.3) becomes

$$\int_{-1}^{1} e^{-i\Phi(z)} = \int_{-\infty}^{+\infty} e^{-i\Psi(\xi)}\frac{dz}{d\xi}d\xi = \int_{-\infty}^{+\infty} \exp\Big[-i(\xi^3/3 - \varsigma\xi)\Big]\frac{dz}{d\xi}d\xi. \tag{C.12}$$

This expression is exact. All the complicated properties are pushed into $dz/d\xi$, which is nevertheless smooth. Since only the vicinity of the saddle points $\xi_\pm$ contributes to the integral, we expand $dz/d\xi$ around these points. At the saddle points, we obtain

$$\Big[\frac{dz}{d\xi}\Big]_{\xi_\pm} = \sqrt{\frac{2a}{b}}\Big(\frac{\varsigma}{b(b-a)}\Big)^{1/4}. \tag{C.13}$$

Therefore, using the integral representation of Airy's function (see Appendix.D, eq(D.3)), we get

$$\frac{1}{2\pi}\int_{-1}^{1} e^{-i\Phi(z)}dz = \sqrt{\frac{2a}{b}}\Big(\frac{\varsigma}{b(b-a)}\Big)^{1/4}\Big[\mathbf{Ai}(-\varsigma) + O(\frac{1}{ab}, \frac{1}{a})\Big]. \tag{C.14}$$

Whence, the integral (C.1) is given by

$$F(s,t) = e^{-\epsilon t - i[\omega_0]t}\sinh(\frac{\pi\Omega}{4\Delta\omega})\sqrt{\frac{2\Omega}{t}}\Big[\frac{\varsigma}{t^2\Delta\omega^2 - \Omega t}\Big]^{1/4}\Big[\mathbf{Ai}(-\varsigma) + O(\frac{1}{\Omega t}, \frac{\Delta\omega}{\Omega})\Big], \tag{C.15}$$

with ς given by (C.8) or (4.9) in the text.

For large $|\varsigma|$ there are asymptotic forms of Airy's function which are given in Appendix D, eqs(D.5) and (D.6). They lead to more transparent forms of the solution as given in the text, (4.10) and (4.11). Without the help of Airy's integral, we can obtain these asymptotic formulae directly by applying the saddle point method in the integral (C.1). However, as one finds from the fact that eqs(4.10) and (4.11) contain $\Omega - t(\Delta\omega)^2$ in the denominator, these formulae cannot be used in the region $\Omega - t(\Delta\omega)^2 \sim 0$; i.e., $\varsigma \sim 0$. (This zero of the denominator is not cancelled by the numerator in contrast to (C.15).) In fact, $\varphi''(p_1)$ vanishes there and the saddle point method fails. Nevertheless, this region is the most important because the maximum amplitude occurs there. This is the reason that we did not employ the saddle point method in this appendix.

Appendix D. Airy's Function

We summarize some useful formulae for the Airy's function $\mathbf{Ai}(-\varsigma)$. The most formulae are taken from ref.6. See it for detail.

The second order linear differential equation

$$\frac{d^2f}{d\varsigma^2} + \varsigma f = 0 \tag{D.1}$$

has two independent solutions, which are oscillatory for $\varsigma > 0$ and exponential for $\varsigma < 0$. (This is easily seen qualitatively by comparing $d^2f/d\varsigma^2 + const. \times f = 0$.) The one which decays exponentially as $\varsigma \to -\infty$ is denoted by $\mathbf{Ai}(-\varsigma)$. (We changed the sign of the argument for our purpose.) It is plotted in Fig.14. It can be expressed by the Bessel functions of order one third as

$$\begin{aligned} \mathbf{Ai}(-\varsigma) &= \frac{\sqrt{\varsigma}}{3}\Big[J_{1/3}(\frac{2}{3}\varsigma^{3/2}) + J_{-1/3}(\frac{2}{3}\varsigma^{3/2})\Big] \qquad (\varsigma > 0) \\ &= \frac{1}{\pi}\sqrt{\frac{-\varsigma}{3}}K_{1/3}(\frac{2}{3}|\varsigma|^{3/2}) \qquad (\varsigma < 0). \end{aligned} \tag{D.2}$$

As one can see from the differential equation, $\mathbf{Ai}(-\varsigma)$ is an entire function, although eq(D.2) looks ugly. It has an integral representation, called Airy's integral;

$$\mathbf{Ai}(-\varsigma) = \frac{1}{2\pi}\int_{-\infty}^{+\infty}\exp\Big[i(\frac{t^3}{3} - \varsigma t)\Big]dt = \frac{1}{\pi}\int_0^{\infty}\cos(\frac{t^3}{3} - \varsigma t)dt \qquad (-\infty < \varsigma < \infty). \tag{D.3}$$

The Taylor expansion at the origin is

$$\begin{aligned} \mathbf{Ai}(-\varsigma) &= \frac{1}{2\sqrt{3}\pi}\sum_{k=0}^{\infty}(-1)^k\Big[\frac{\Gamma(k+1/3)}{\Gamma(3k+1)}3^{k+1/3}\varsigma^{3k} + \frac{\Gamma(k+2/3)}{\Gamma(3k+2)}3^{k+2/3}\varsigma^{3k+1}\Big] \\ &= \frac{1}{3\pi}\sum_{n=1}^{\infty}\frac{\Gamma(n/3)}{\Gamma(n)}\sin(\frac{n\pi}{3})3^{n/3}\varsigma^{n-1} \qquad |\varsigma| < \infty. \end{aligned} \tag{D.4}$$

The asymptotic forms for $|\varsigma| \to \infty$ are

$$\mathbf{Ai}(-\varsigma) = \frac{1}{2\sqrt{\pi}}(-\varsigma)^{-1/4}\exp\Big[-\frac{2}{3}(-\varsigma)^{\frac{3}{2}}\Big] \times (1 + O(|\varsigma|^{-3/2})) \qquad -\pi < \arg(-\varsigma) < \pi \tag{D.5}$$

$$= \frac{1}{\sqrt{\pi}}\varsigma^{-1/4}\Big[\sin\Big(\frac{2}{3}\varsigma^{\frac{3}{2}} + \frac{\pi}{4}\Big) + O(|\varsigma|^{-3/2})\Big] \qquad -\frac{2}{3}\pi < \arg\varsigma < \frac{2}{3}\pi. \tag{D.6}$$

The value at the origin is

$$\mathbf{Ai}(0) = \frac{3^{-2/3}}{\Gamma(2/3)} = 0.3550 \qquad \text{and} \qquad \Big[\frac{d\mathbf{Ai}(-\varsigma)}{d\varsigma}\Big]_{\varsigma=0} = \frac{3^{-1/3}}{\Gamma(1/3)} = 0.2588 \tag{D.7}$$

There are infinite number of zeroes of $\mathbf{Ai}(-\varsigma)$ on the positive real axis. The first few are

$$\varsigma = 2.338, \quad 4.088, \quad 5.521, ... \tag{D.8}$$

and the n-th zero for large n is given by

$$\varsigma_n = [\frac{3\pi}{8}(4n-1)]^{2/3} + O(n^{-4/3}). \tag{D.9}$$

The maximum of $\mathbf{Ai}(-\varsigma)$ on the real axis is

$$\mathbf{Ai}(-\varsigma) = 0.5357, \qquad \text{at} \quad \varsigma = 1.019. \tag{D.10}$$

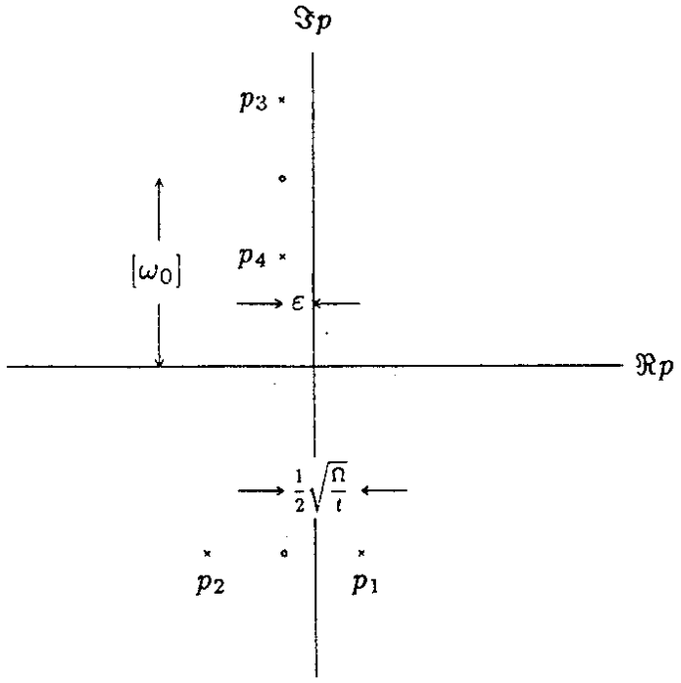

Fig.1 The singularities (circles) and the saddle points (crosses) of the integrand of eq(3.8) in the complex p-plane.

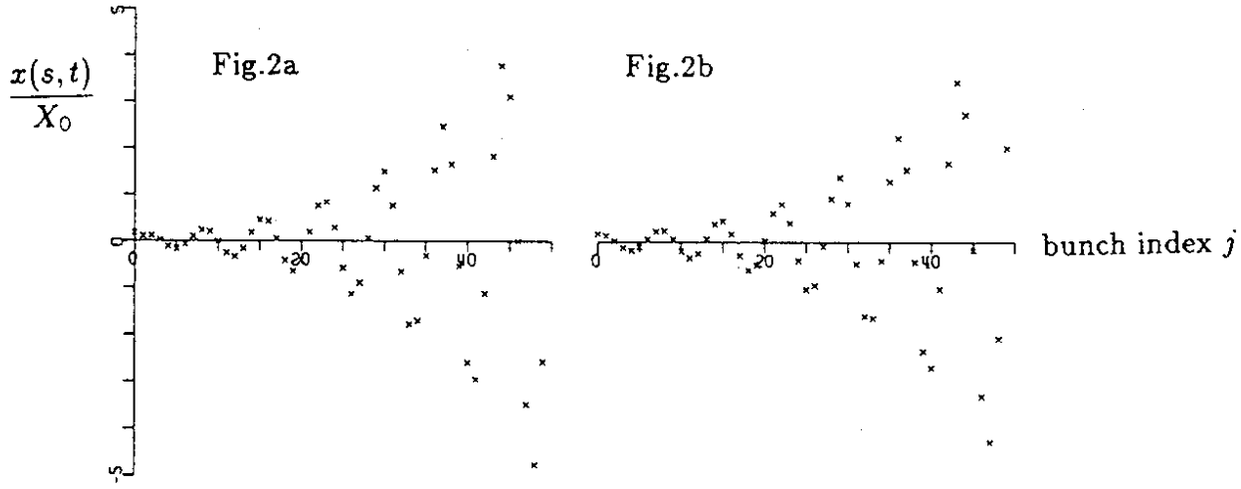

Fig.2 Beam breakup in the absence of the frequency spread. Plotted is $x_j(s)/X_0$ by the tracking (2a) and by the formula (3.22) (2b) as a function of the bunch index j. At s=200m. Other parameters are given in Section 3.

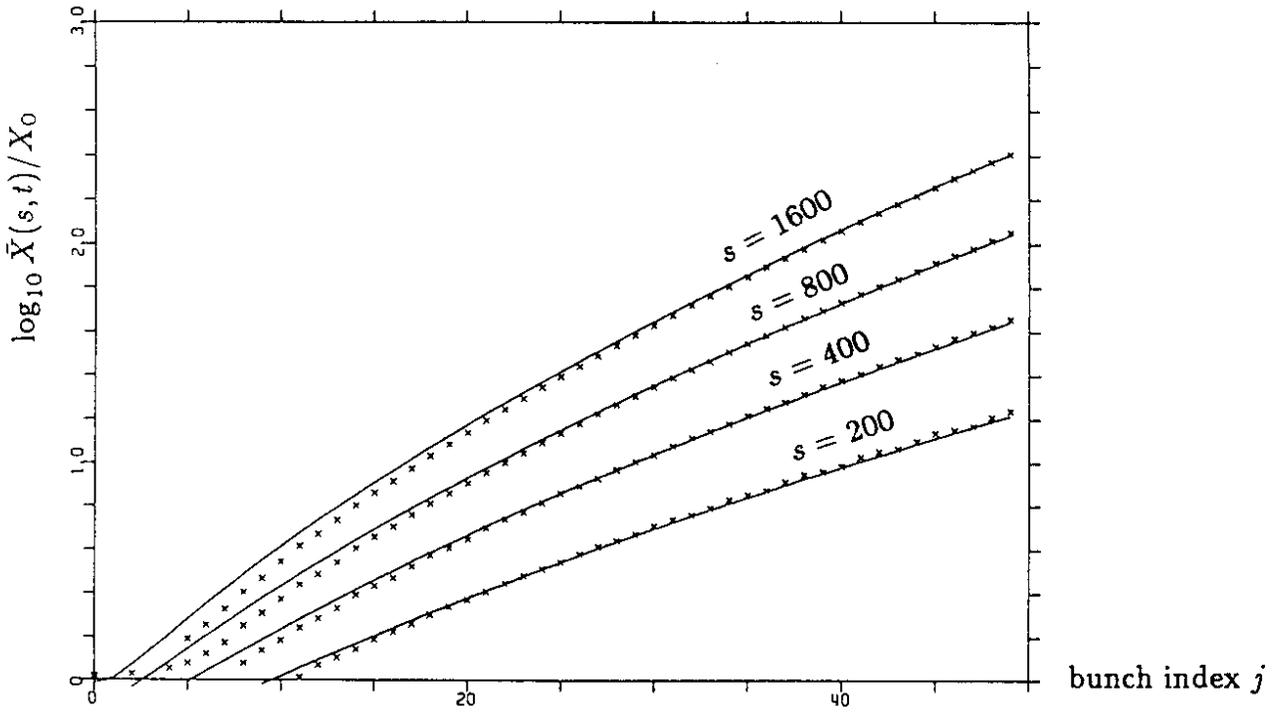

Fig.3 The growth of the oscillation amplitude in the absence of the frequency spread. Here, $\log_{10}(\bar{X}(s,t)/X_0)$ is plotted as a function of t for some fixed values of s. The crosses and the solid lines are according to the tracking and the formula (3.23), respectively.

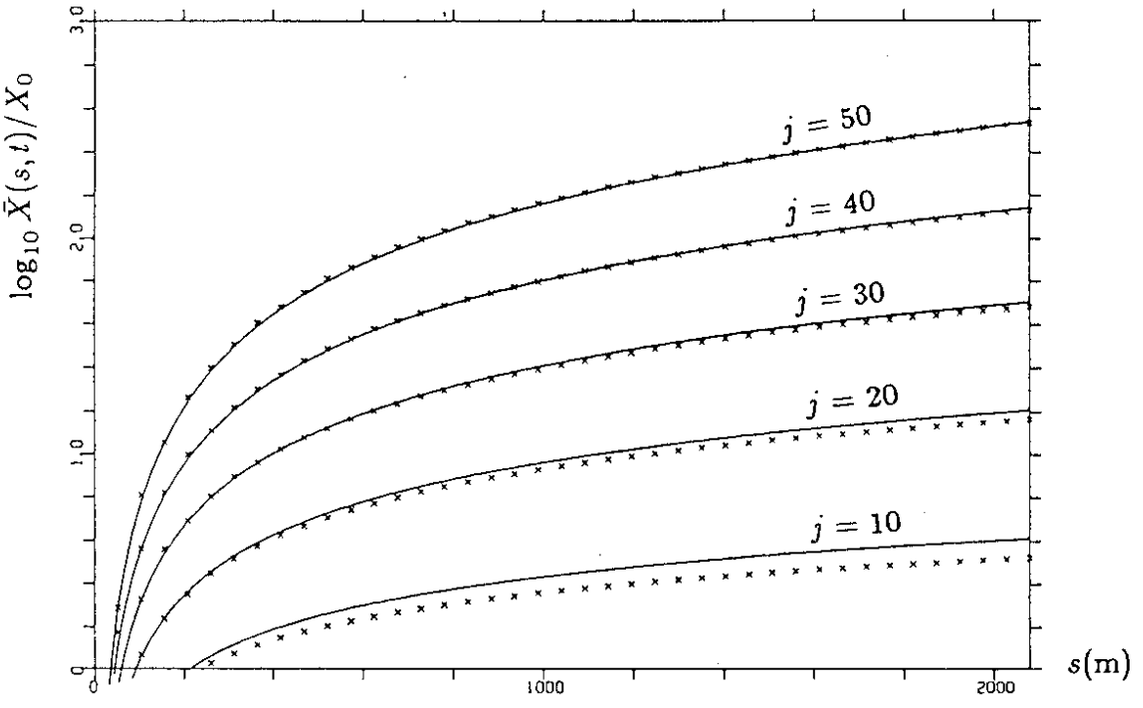

Fig.4 The same as in Fig.3 but as a function of s for some fixed t (bunch index).

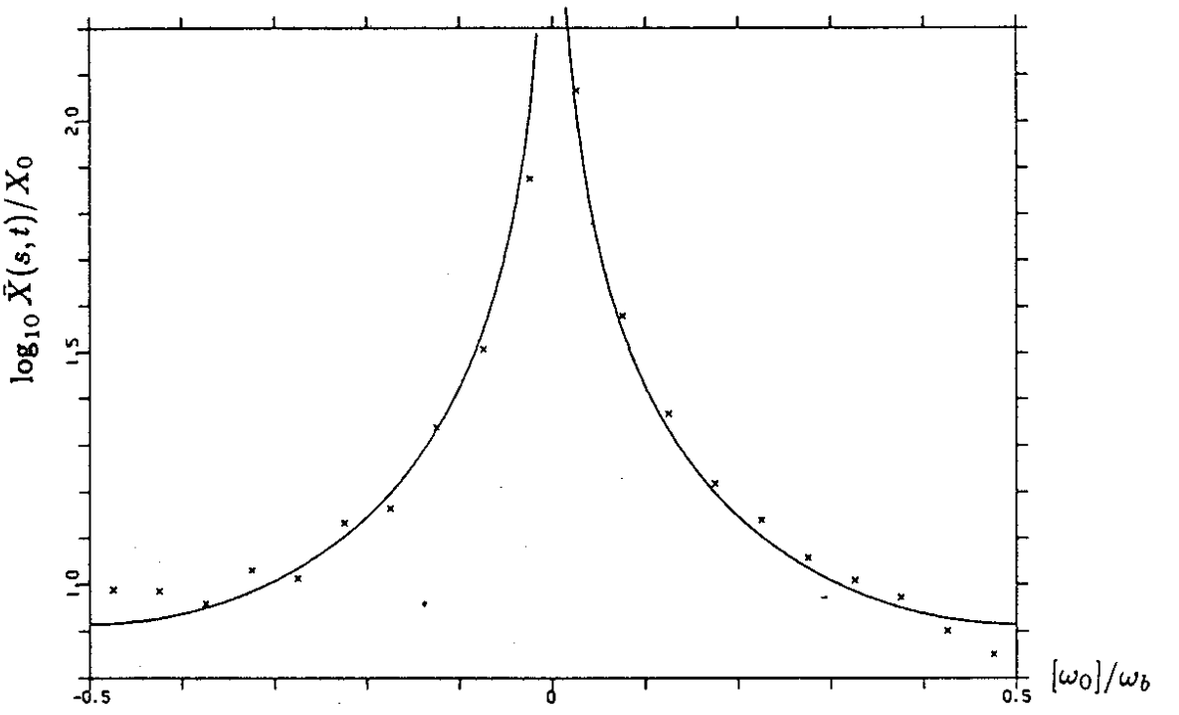

Fig.5 The resonance between the mode frequency and the bunch arrival frequency in the absence of the frequency spread. The horizontal axis is $[\omega_0]/\omega_b$ and the vartical $\log_{10}(\bar{X}(s,t)/X_0)$ ($s = 1000m$, 50-th bunch). Eq(2.16) (whole beam offset) is used as the initial condition.

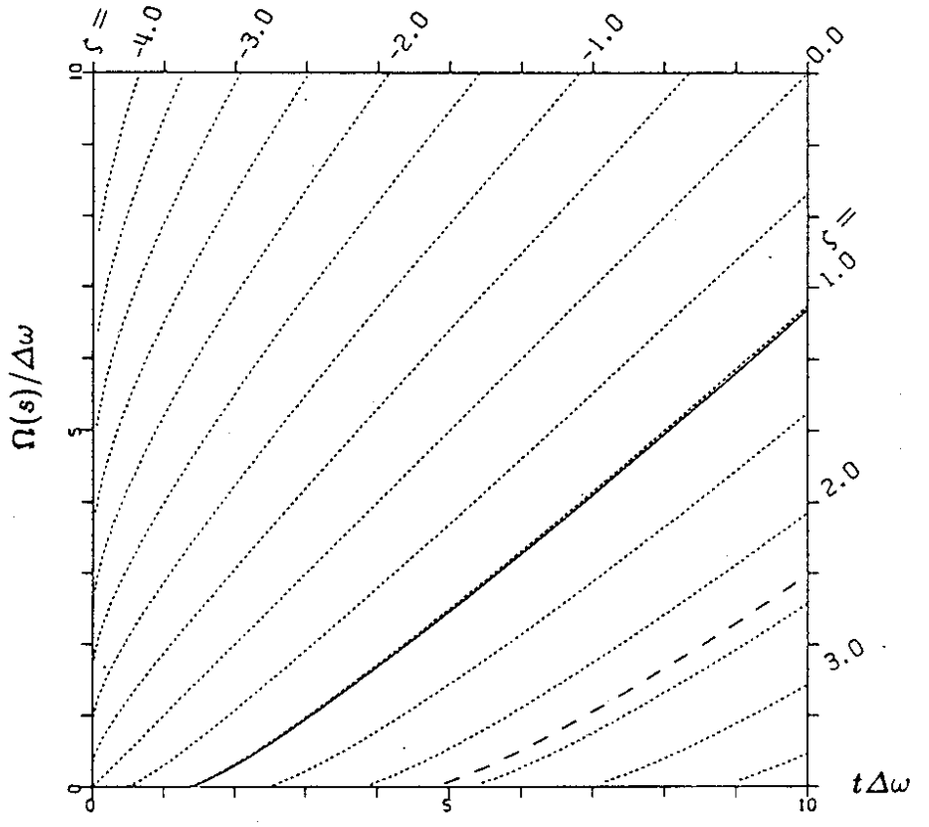

Fig.6 The relation between $\Omega(s)$, t and ς. The horizontal axis is $t\Delta\omega$ and the vertical $\Omega(s)/\Delta\omega$. The dotted lines are the contours of constant ς. The solid line and the dashed lines are the maximum and zeroes of $\mathbf{Ai}(-\varsigma)$.

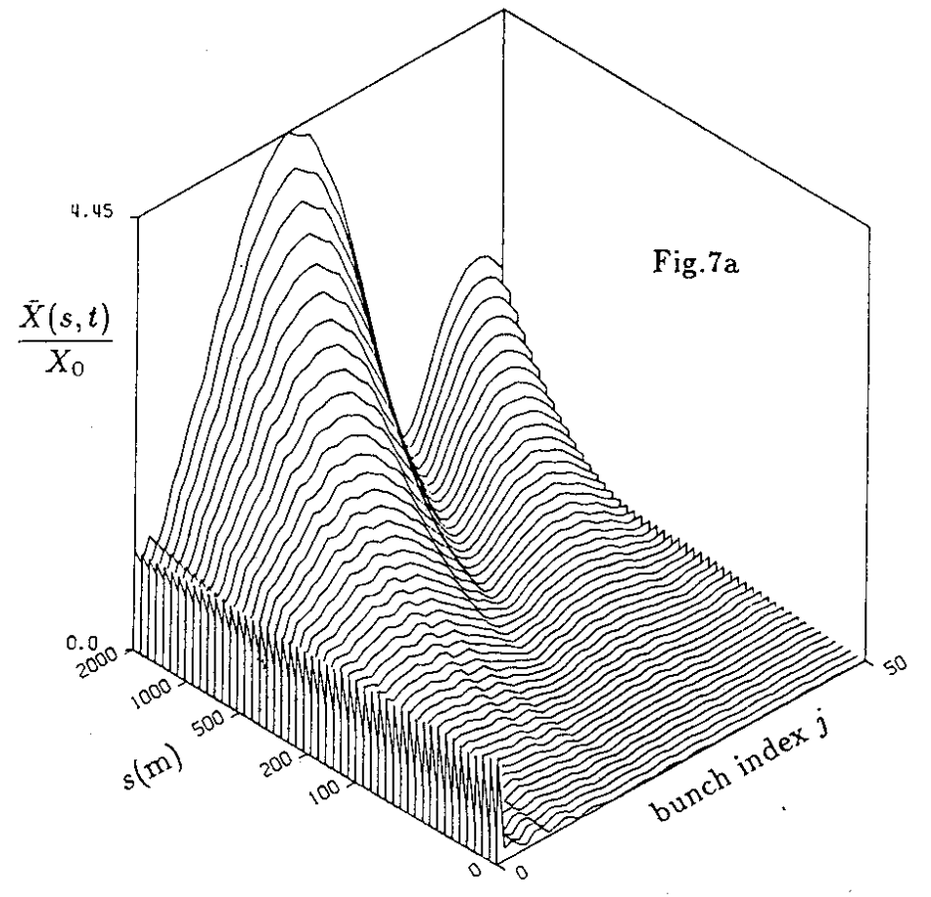

Fig.7a

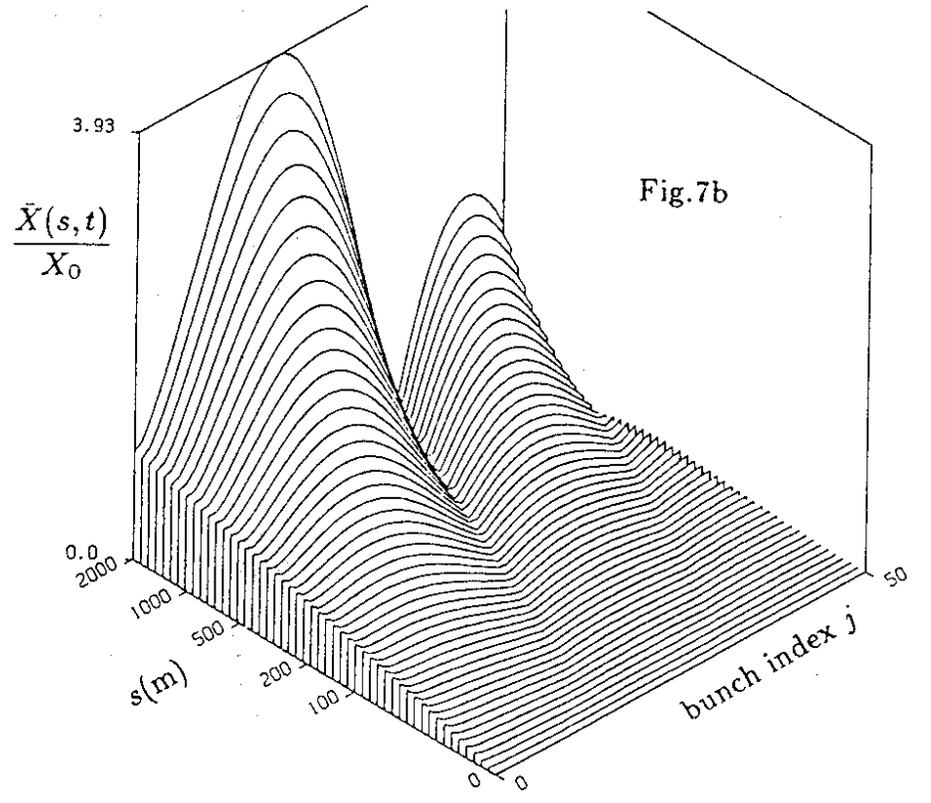

Fig.7b

Fig.7 The amplitude $|\bar{X}(s,t)/X_0|$ as a function of s and t, by the tracking (7a) and the formula (4.8) (7b) in the presence of a frequency spread. The s-axis is scaled linear in $\Omega(s)$.

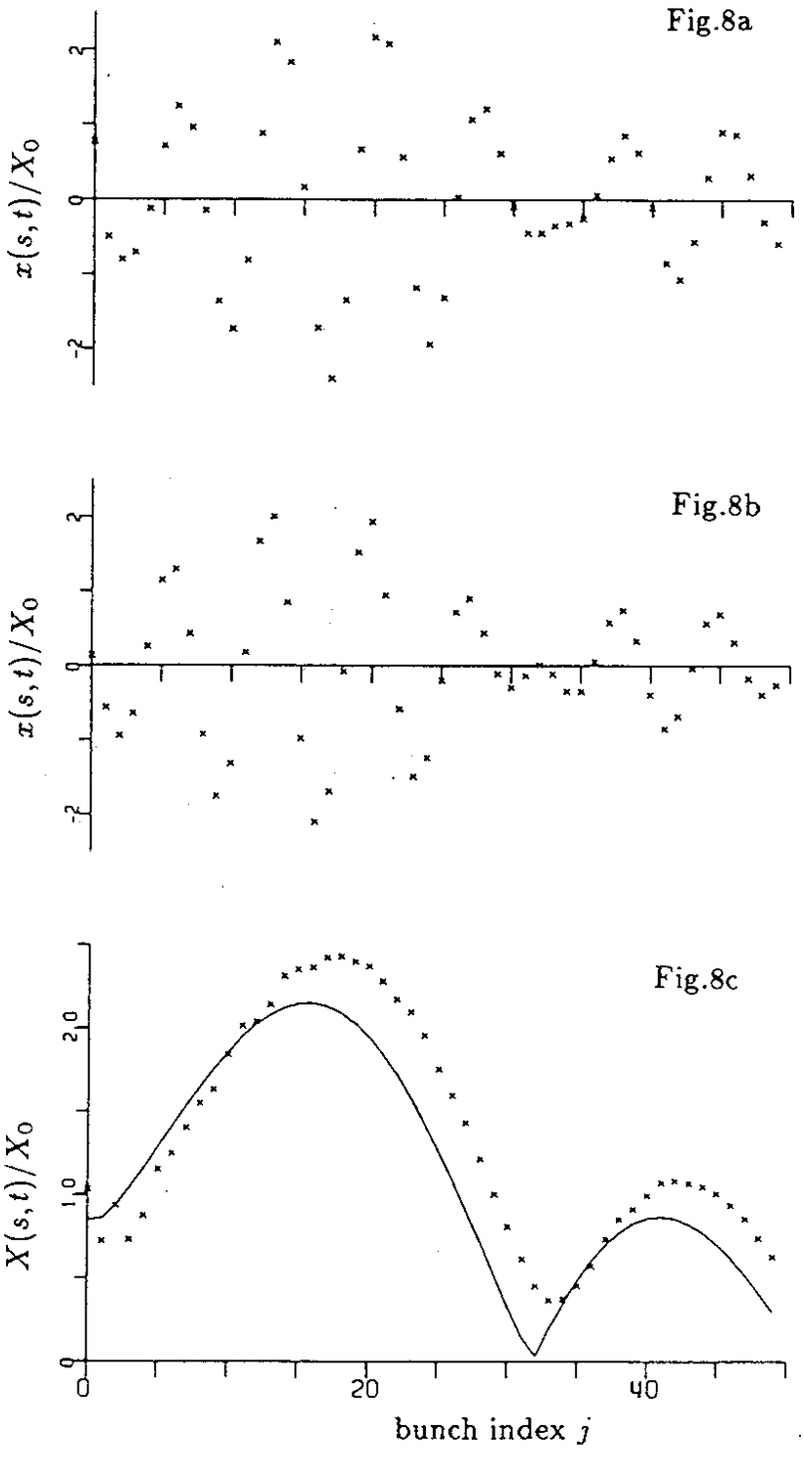

Fig.8 The behavior of the beam as a function of t (bunch index j) for fixed s (1000m) in the presence of a frequency spread. Fig.8a and 8b show $x(s,t)/X_0$ by the tracking and the formula (4.7), respectively. Fig.8c is the amplitude $\log_{10}(\bar{X}(s,t)/X_0)$.

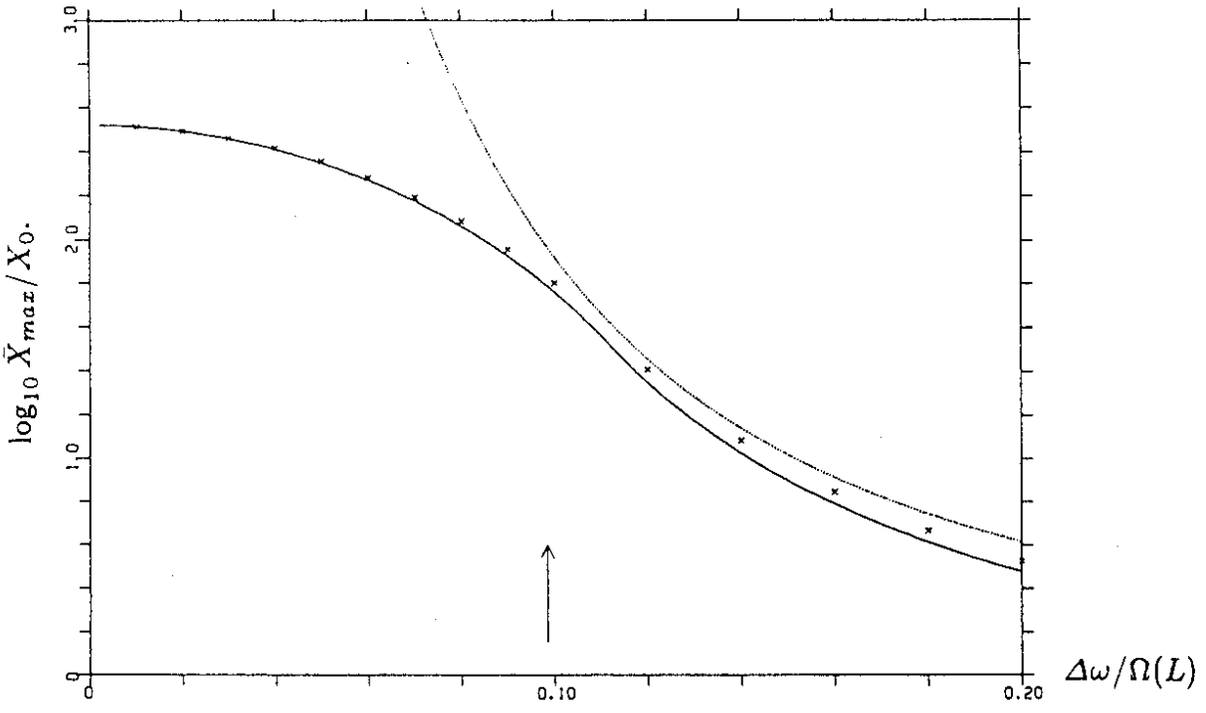

Fig.9 The maximum amplitude X_{max}/X_0 as a function of the frequency spread $\Delta\omega$ ($X_{max} = \max_{0<s<L, 0<t<T} X(s,t)$). The crosses show the traking results. The solid line is the maximum of the formula (4.8) and the dotted line is the simplified formula (4.14). The location where (4.15) holds is indicated by an arrow. Eq(4.14) applies under the condition (4.12); i.e., to the right of the arrow.

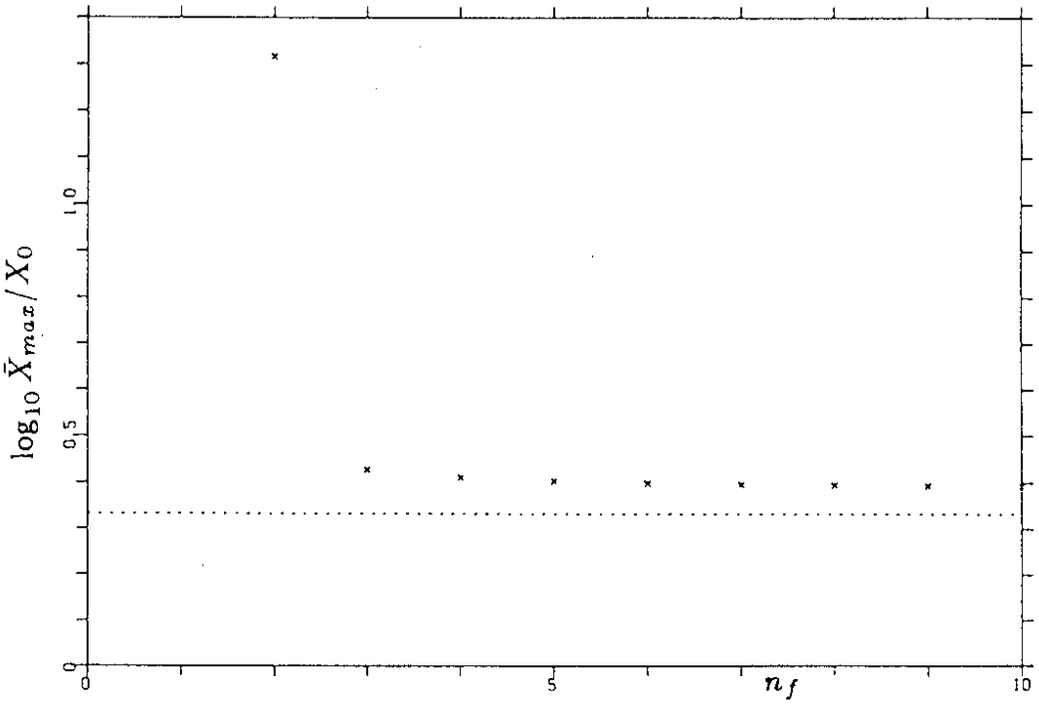

Fig.10 The dependence of X_{max} on the number of mode frequencies n_f. The total spread is $\Delta\omega/2\pi = 6.0$MHz. The vertical axis is $\log_{10} \bar{X}_{max}/X_0$.

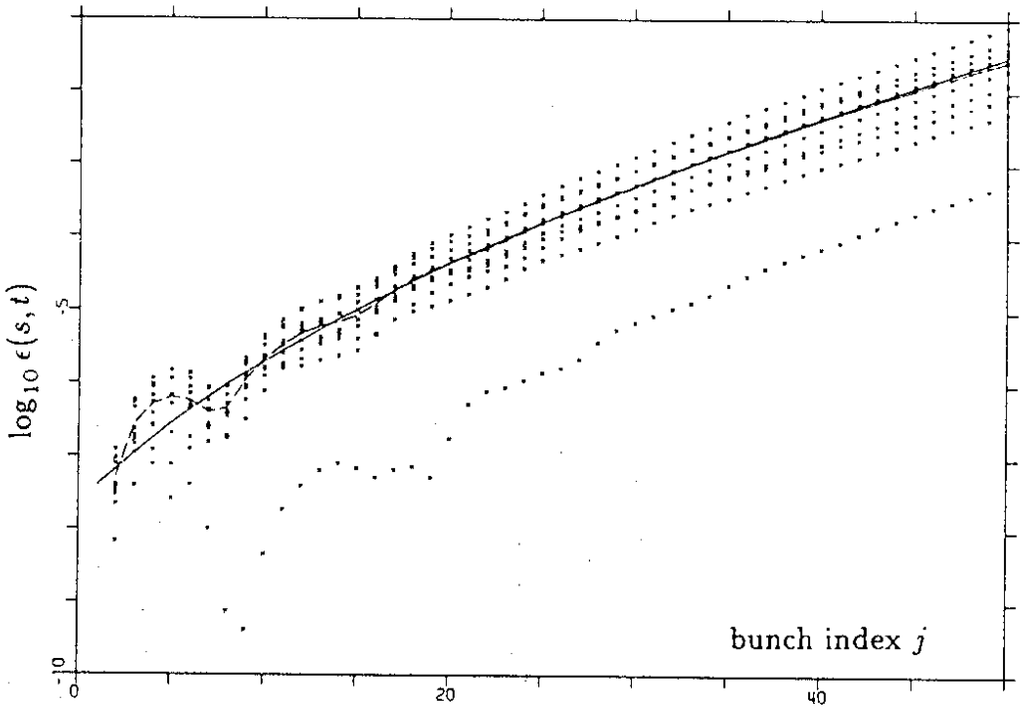

Fig.11 The misalignment effect in the absence of the frequency spread. The normalized Courant-Snyder invariant $\log_{10}\epsilon(s,t)$ (in meter radian) is plotted against the bunch index for fixed s (=2000m). The crosses are the results of the tracking for ten different sets of random numbers and the dashed line is their average. The solid line shows the formula (5.14).

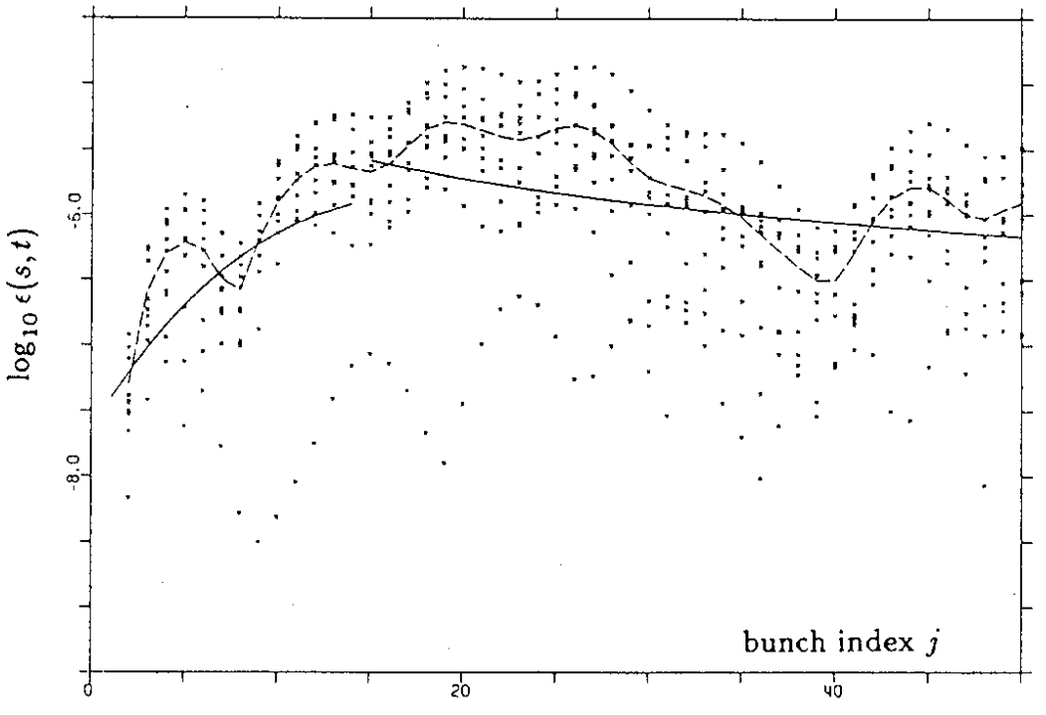

Fig.12 The misalignment effect in the presence of the frequency spread of 6MHz. The solid line on the left representse the formula (5.23) and that on the right (5.25). Others are the same as in Fig.11.

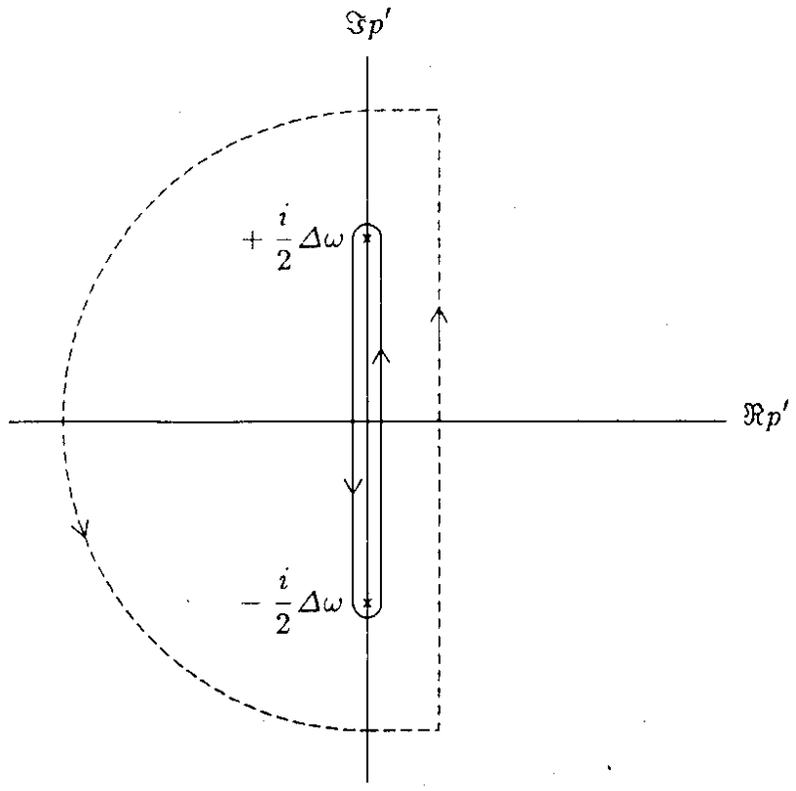

Fig.13 The deformation of the integration path in eq(C.2) in the complex p'-plane.

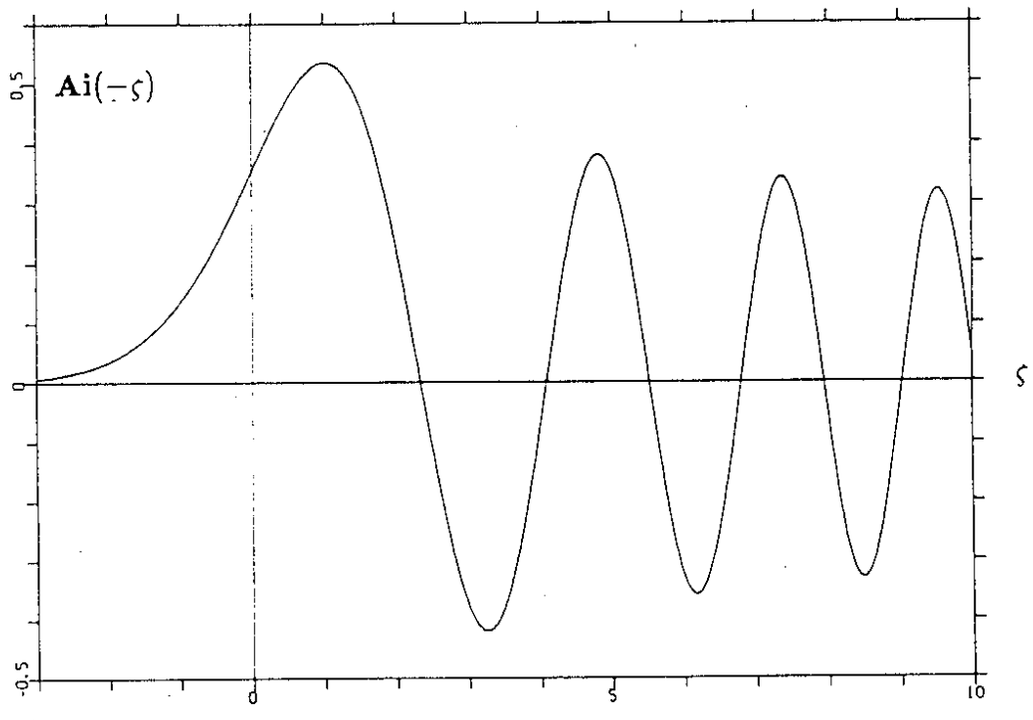

Fig.14 Airy's function $\mathbf{Ai}(-\varsigma)$.